



Linearisation of an FM-CW 94.5 GHz

Millimeter-Wave Radar

WM de Wit

Thesis presented in partial fulfilment of the requirements
for the degree of **Master of Science in Engineering (Electronic)**
at the Department of Electrical and Electronic Engineering
of the University of Stellenbosch.

Supervisor: Prof. J.B. de Swardt

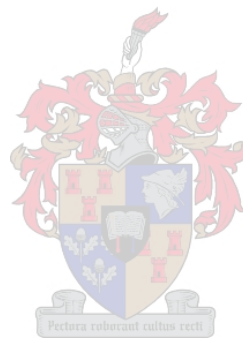
April 2006

Declaration

“I, the undersigned, hereby declare that the work contained in this thesis is my own original work, unless stated otherwise, and that I have not previously in its entirety or in part submitted it at any university for a degree.”

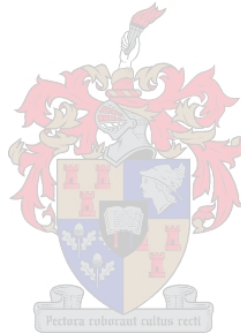
Wynand Marius de Wit

December 2005



Summary

The topic of millimeter wave radar systems is introduced. These radars are used in a wide range of applications in both the aviation and automotive field due to the resolution advantages which MMW systems have above their counterparts. MMW components are studied and characterised to improve on an existing linearisation technique. Different possible linearisation techniques are discussed and compared to choose the best possible technique for this application. This technique was developed and implemented in the existing system.



Opsomming

Hierdie is `n inleiding tot die onderwerp van millimeter golf radars. Hierdie radars word in verskeie toepassings in beide die lugvaart en motorbedryf gebruik. Millimeter golf komponente is ondersoek en gekarakteriseer om `n bestaande lineariseringstegniek te verbeter. Verskeie tegnieke is ondersoek en vergelyk om die beste een te kies vir die toepassing. Die tegniek is ontwikkel en geïmplementeer in die stelsel.



Contents

Summary	iii
Opsomming	iv
Acknowledgements	ix
1 Introduction	1
1.1 Thesis Structure	2
2 Background on MMW-Radars	4
2.1 Introduction to MMW-Radars	4
2.2 Fundamentals of MMW Radar Systems	6
2.3 MMW Radar Characteristics	7
2.4 Fundamental Design Considerations	12
2.4.1 Functional Elements	12
2.4.2 Environment	16
2.4.3 Measures of Performance	20
2.5 Applications of MMW-Radars	22
2.5.1 Automotive Applications	23
2.5.2 Aviation Applications	23
2.6 Characteristics of basic components	24
2.6.1 Antenna	25
2.6.2 Quadrature (90°) Hybrid	27
2.6.3 Coupler	28

2.6.4 Dielectric Resonator Oscillator (DRO)	28
2.6.5 Harmonic Mixer	29
2.6.6 Isolator	30
2.6.7 Voltage Controlled Oscillator (VCO).....	31
2.7 Conclusion	33
3 Factors influencing the accuracy of the system	34
3.1 The Doppler Effect	34
3.2 CW Radar	35
3.3 Frequency-Modulated CW Radar	37
3.4 Range and doppler measurement.....	37
3.4.1 Modulation Frequency.....	41
3.4.2 Deviation Frequency.....	45
3.5 Linearity of the transmitted signal.....	46
3.5.1 Influence of nonlinear modulation in the time domain	48
3.5.2 Influence of nonlinear modulation in the frequency domain.....	48
3.6 Conclusion	49
4 Linearization Techniques	50
4.1 Definition of VCO linearization techniques	50
4.2 Open Loop Linearization Technique	51
4.3 Closed loop linearization technique using a frequency discriminator.....	52
4.3.1 Digital frequency discriminator technique	53
4.3.2 Analogue frequency discriminator technique	56
4.4 Phase Lock Loop with Direct Digital Synthesizer	58
4.5 Conclusion	58
5 Phase Lock Loop using a Direct Digital Synthesizer	60
5.1 Basic Principles of a PLL	60
5.1.1 PLL Operation	60
5.1.2 Lock and Capture.....	62
5.1.3 The capture transient.....	63
5.1.4 Effect of the Loop Filter	64

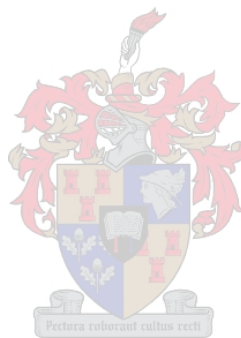
5.2	Component characteristics in a PLL.....	65
5.2.1	Phase Detectors.....	65
5.2.1.1	Phase Detector Gain	66
5.2.1.2	Digital Phase Detectors.....	67
5.2.1.3	XOR.....	68
5.2.1.4	Two state Phase Detectors.....	69
5.2.1.5	Phase-Frequency Detectors	70
5.2.2	Voltage-Controlled Oscillator (VCO).....	71
5.2.3	Loop Filters.....	71
5.2.4	Amplifier.....	71
5.3	Determining PLL model parameters	71
5.3.1	Mathematically defining PLL operation.....	72
5.3.2	Unlocked state ($\omega_1 \neq \omega_0$).....	72
5.3.3	Locked state ($\omega_1 = \omega_0$).....	73
5.3.4	Modelling the PLL system with various low-pass filters	75
5.4	Low Pass Filter Design.....	75
5.4.1	Zero order filter.....	75
5.4.2	First-order filter	76
5.4.3	First order lag-lead filter.....	77
5.4.4	Second- and Higher-Order Filters.....	79
5.5	Conclusion	79
6	System Implementation	80
6.1	Phase Detector	80
6.2	Harmonic Mixer.....	82
6.3	Amplifier Implementation	82
6.4	DDS Implementation.....	84
6.5	Filter Implementation	85
6.6	Microcontroller Implementation.....	88
6.7	Implementation and Measurements of PLL	88
6.8	Conclusion	93



7 Conclusions and recommendations 94
7.1 Conclusion94
7.2 Recommendations for future research.....95

Bibliography 96

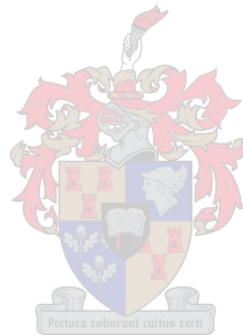
Appendix A Range resolution as a function of slope linearity ... 98



Acknowledgements

I would like to thank the following people for their support on this thesis

- First and foremost, thanks be to God for the help and guidance that could only be provided by Him. May the thesis serve to praise His Name.
- My wife to be, Marilene Taljaard, for her patience and support through this difficult time. The thesis would not be possible without your support.
- My family, Mom and Dad, for their support through the years of studies.
- Prof. Johann B. de Swardt for his patience in guiding me in my work on the thesis.
- Vitto Basso for his help and guidance with the existing system.
- And lastly to all my friends and work colleagues for all their support and well wishes.



1 Introduction

The Millimeter-Wave (MMW) region of the electromagnetic spectrum has received increased interest in recent years due to the significant advances in the development of components of transmitters, receivers, devices and components in system applications in fields such as radar radiometry, remote sensing, missile guidance, radio astronomy, communications and spectroscopy.

One major advantage of MMW applications above its counterparts is the excellent resolution and hence the accuracy obtained in measurements. This advantage is very important in system applications such as missile terminal guidance seekers, airborne surveillance sensors, altitude meters and anti-collision systems in the aviation and automotive sector.

The accuracy and performance of MMW systems is greatly dependant on the linearity of the system.

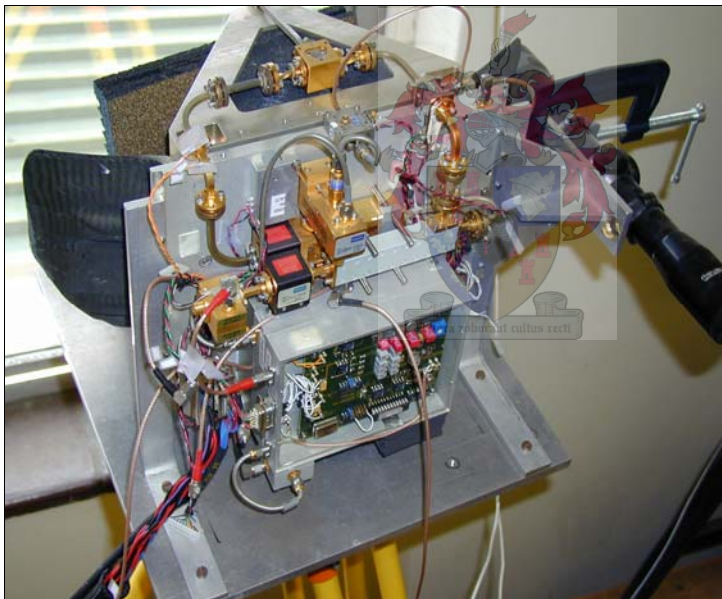


Figure 1.1 Photo taken of MMW Radar.

Figure 1.1 shows the complexity of the existing MMW system. In order to improve the

linearity a good understanding and insight of the system is needed. A lot of time was spent on the measuring and characterization of the components of the system to gain an understanding of the system.

The aim of this work is to improve an existing linearization scheme. The existing linearization scheme implements a Frequency Discriminator (FD) configured in a closed loop feedback system. The improvement in linearity of the system will therefore be dependant on the performance of the Frequency Discriminator. The new system will replace the current Frequency Discriminator with a Phase Frequency Detector and a Direct Digital Synthesizer (DDS) as the reference to the Phase Frequency Detector. The Phase Frequency Detector and DDS will be configured in a closed loop feedback system as a Phase Lock Loop (PLL). The Voltage Controlled Oscillator will therefore be locked to the frequency of the DDS. The linearity of the system will therefore only be dependant on the performance of the DDS.

The following section serves as an outline of the thesis structure.

1.1 Thesis Structure

Thesis structure is as follows:

- Chapter 2 provides an overview on the basic characteristics, fundamentals and design considerations of MMW Radars. Functional elements and the effects of the environment on the performance of MMW Radar systems are discussed. The history of MMW Radar development and the application of MMW Radar in the automotive and aviation industry are discussed. The chapter concludes with characterization of the basic components of the system.
- Chapter 3 introduces the factors influencing the accuracy of the system. The basic operation of a Frequency Modulated Continuous Wave (FMCW) Radar is discussed. The effects of the modulation frequency and deviation frequency is discussed in detail. The chapter concludes with an essential discussion of the effect that linearity has on the performance of the system.
- Chapter 4 introduces the various linearization techniques with an in depth study on the closed loop linearization technique. The advantages and disadvantages of the

techniques are discussed and compared. The chapter concludes with the linearization technique chosen for this thesis.

- Chapter 5 describes the phase lock loop technique using a Direct Digital Synthesizer (DDS). The basic principles of a Phase Lock Loop (PLL) are discussed with a detailed look at the individual components characterizing the PLL and determining PLL model parameters. This chapter concludes with the design considerations of the Low Pass Filter (LPF) of the PLL.
- Chapter 6 describes the system implementation of the linearization technique using the PLL technique. Design and implementation of the PLL is shown. This chapter concludes with measurement results of the implementation.
- Chapter 7 concludes with a summary and recommendations for future work.



2 Background on MMW-Radars

Little was known at the time about the existing system shown in Figure 1.1 . The first aim was to get the system operational. In order to achieve this, a better understanding of the fundamentals and characteristics of MMW-Radar system is necessary. This was done by investigating the effect of the environment on the design and implementation of MMW-Radars, and the characterizing of MMW components.

2.1 Introduction to MMW-Radars

The MMW region of the electromagnetic spectrum is generally defined as the frequency from 30 GHz to 100 GHz (wavelengths between 1cm and 1mm).

One characteristic of the MMW frequency is that for a given physical antenna size (aperture) the antenna beam width is smaller and the gain is higher than at microwave frequencies. Therefore, to obtain a high gain or smaller beam width, a much smaller antenna may be used. This is a very important characteristic in many system applications where size and weight of the hardware are constrained, such as for missile terminal guidance seekers and airborne surveillance sensors.

In general, atmospheric propagation effects dominate design consideration relating to many MMW-radar applications. Terrestrial systems designing to prevent signal “overshoot” in range may operate at a frequency of high atmospheric absorption to gain a specific degree of covertness [1]. Typical values of atmospheric attenuation are shown in Figure 2.1 for propagation at sea level and at an altitude of 4km.

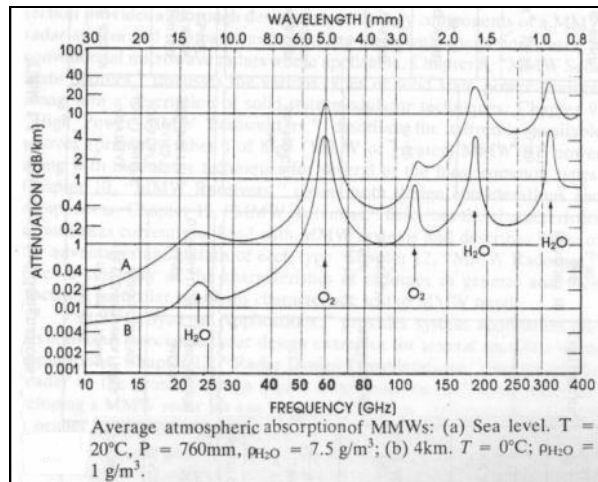


Figure 2.1 Typical values of atmospheric attenuation [1].

The maximum absorption regions are called “walls” and the minima regions are called “windows”. These maxima and minima regions are the cause of atmospheric constituents such as oxygen and water vapour. MMW systems are superior over optical and infrared systems for penetration of smoke, fog, haze, dust, clouds and other adverse environments. The limitations and capabilities of MMW radar will be discussed in section 2.3. Table 2.1 provides a summary of the early MMW technology milestones.

Table 2.1 Significant MMW technology milestones [1].

Date	Event
1936	First resonant spectral measurement (ammonia inversion at 27.3 GHz), by Cleeton and Williams.
1937	Invention of the klystron oscillator by Russell and Sigurd Varian.
1939	Invention of the cavity magnetron by Boot and Randall.
1942	Development of the crystal mixer at Bell Laboratories.
1946	First MMW magnetron developed.
1947	First K_a -band radars (AN/SPS-7 surface radar developed by the US Navy, and AN/TPQ-6 cloud height measuring radar developed by Bendix for the US Air Force)
1960	Development of MMW klystrons and magnetrons by US Army Signal Corps Laboratories.
1962	Gunn effect discovered in GaAs by J.B Gunn.
1964	IMPATT oscillator developed separately at Bell Laboratories and in the Soviet Union.

2.2 Fundamentals of MMW Radar Systems

Full understanding of the operational characteristics of MMW-Radar requires an appreciation for the location of MMW band within the electromagnetic spectrum and the resulting effects on the propagation of MMW energy. Figure 2.2 illustrates the electromagnetic spectrum and identifies the region of conventional radar operation, along with standard radar operating band designations.

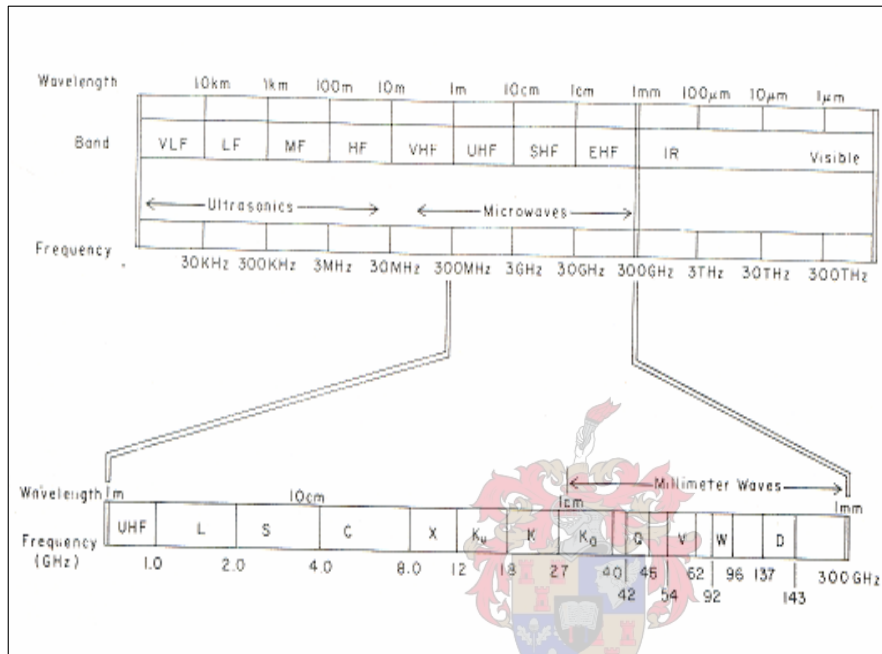


Figure 2.2 Electromagnetic spectrum with radar band designations [1].

Most applications of radar involve achieving as long a detection range as possible; consequently, radar research and development has been concentrated in the areas of low attenuation at the MMW window frequencies of 35 GHz, 95 GHz, 140 GHz and 220 GHz [1]. Water vapour and oxygen molecule electromagnetic interaction resonances provide regions of abnormally large absorption which, in turn, cause the relative maxima or walls occurring at approximately 60 GHz, 120 GHz and 180 GHz. Radars have also been

developed at these frequencies to take advantage of the covertness provided by the high atmospheric absorption, and to operate in exoatmospheric space where atmospheric absorption does not exist. Figure 2.3 provides a representation of the clear-air atmospheric attenuation between 3 cm and 0.3 μm wavelengths.

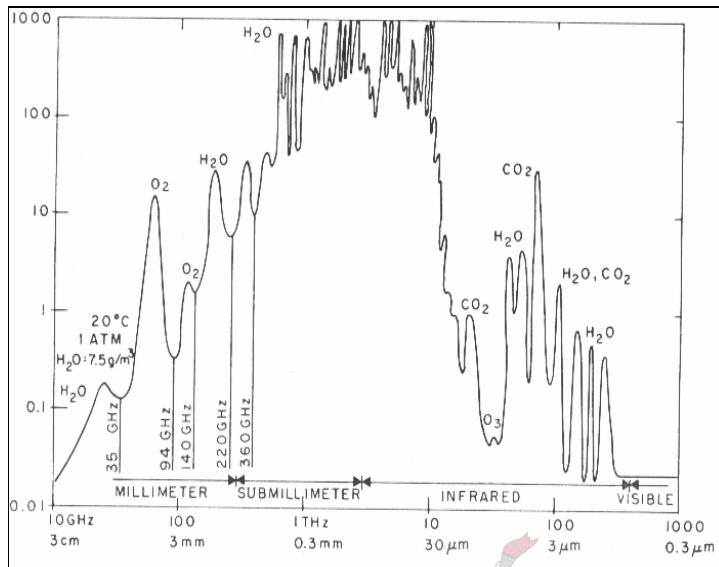


Figure 2.3 Clear weather atmospheric attenuation [1].

Many of the key operational features of MMW radar are directly dictated by the atmospheric propagation characteristics discussed above and will be discussed in the following section.

2.3 MMW Radar Characteristics

As Table 2.2 indicates, MMW radar offers significant operational advantages when compared to microwave radar, especially in the area of high angular resolution resulting from smaller antenna beamwidths for a fixed antenna aperture size.

Table 2.2 MMW Radar System Trade off Considerations [1].

<i>Advantages</i>	<i>Limitations</i>
Physically Small Equipment	Component Cost High
Low Atmospheric Loss (Compared to IR and Visual Wavelengths)	Component Reliability and Availability Low
High Resolution Angular Doppler Imaging Quality Classification	Short Range (10-20 km) Weather Propagation (Compared to Microwave Frequencies)
Small Beamwidths High Accuracy Reduced ECM Vulnerability High Antenna Gain	
Large Bandwidth High Range Resolution Spread Spectrum ECCM Doppler Processing	

The half-power (3 dB) beamwidth, θ , of an antenna, as illustrated in Figure 2.4 , in the plane corresponding to the antenna dimension, is related to the operating frequency.

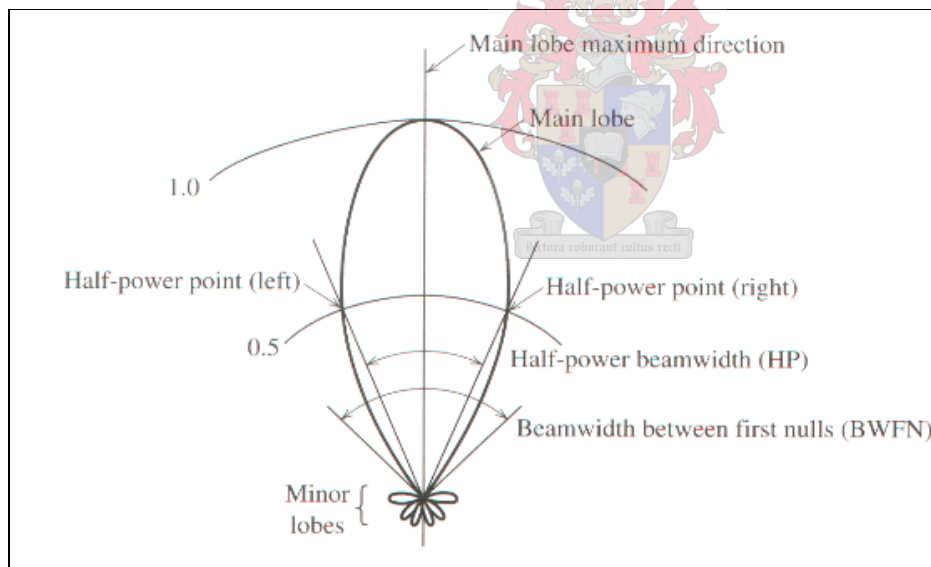


Figure 2.4 A typical power pattern polar plot of a diffraction limited antenna [3].

The relation between the half-power beamwidth and the operating frequency is given by the following equation [2].

$$\Theta = \frac{k\lambda}{l} \text{ radians} \quad (2-1)$$

where

k = constant ($4/\pi$ for -25 dB sidelobes),

λ = wavelength,

l = aperture dimension.

Solving equation (2-1) for several aperture dimensions and frequencies yields Table 2.3, which provides antenna beamwidth (in degrees) as a function of radar operating frequency.

Table 2.3 Antenna Beamwidth versus Frequency [1].

Aperture Size (m)	10 GHz	35 GHz	95 GHz	140 GHz	220 GHz
0.01	219	62.5	23.1	15.6	9.9
0.1	21.9	6.3	2.3	1.6	1
1	2.2	0.63	0.23	0.16	0.1

The availability of significant smaller antenna beamwidth results in several of the most important operational advantages to MMW radar. Among the more important of these are:

a) High Antenna Gain with Small Aperture



Skolnik [2] gives the gain, G , of an antenna relative to an isotropic radiator as

$$G = \frac{4\pi A_e}{\lambda^2} \quad (2-2)$$

Where A_e = effective area of antenna aperture. Thus, the gain of an antenna increases in proportion to the frequency of operation squared, again for a fixed aperture.

b) High Angular Tracking Accuracy

Radar's angular tracking accuracy is directly related to its antenna beamwidth [1], θ , as shown below for a thermal noise limited case:

$$\sigma_t = \frac{(k_t \Theta)}{[(S/N)_n]^{1/2}} \quad (2-3)$$

where

σ_t = root-mean-square (rms) angle tracking error,

k_t = constant depending on type of tracking,

(S/N) = signal-to-noise ratio at receiver input,

n = number of pulses integrated,

Θ = half-power beamwidth, (2-1).

Thus, all other things equal, MMW radar can expect a reduction in tracking errors when compared to lower frequency radar, as a direct result of smaller antenna beamwidth.

c) Reduced Electronic Countermeasures (ECM) Vulnerability

Smaller antenna beamwidths provide less opportunity for a jammer to inject energy into the radar's main beam and thus reduces the radar's susceptibility to jamming.

d) Reduction in Multipath and Ground Clutter at low Elevation Angles

MMW radar with small beamwidth will typically have less ground intercept than lower frequency radar with larger beamwidths. Since ground intercept is reduced, multipath propagation conditions and ground clutter are correspondingly reduced.

e) Improved Multiple Target Discrimination and Target Identification

Again, a radar's ability to separate multiple, closely-spaced targets and to provide information for target identification is closely coupled to its resolution. Thus, MMW radars inherent advantages in these areas.

In addition to the high angular resolution of a MMW radar, another important characteristic is the radar's ability to measure and resolve target motion through the Doppler effect. Any target motion in the radar's beam will cause a shift in the received signal frequency in accordance with the following relationship [1].

$$f_d = \frac{2V_r}{\lambda} \quad (2-4)$$

where

f_d = Doppler frequency,

V_r = radial target velocity,

λ = wavelength of transmitted signal.

Table 2.4 presents the Doppler frequency shift for several radar operating frequencies. For a target having a 30m/s radial velocity with respect to the radar, a radar operating at 10 GHz (X-band) would experience a 2 kHz frequency shift (i.e., the received signal frequency would be 10 000 002 kHz for a target radially approaching the radar). 95 GHz radar observing the same target would experience a 19 kHz frequency shift. Such large Doppler shifts from relatively slow moving targets provide the capability for increased target detection and perhaps recognition of such target features as skin vibration, and second and higher order velocity signatures.

Table 2.4 MMW Radar Characteristics: Doppler Frequency Properties [1].

<i>Radar Frequency</i> (GHz)	<i>Doppler Shift</i> (Hz/m/s)
10	66.7
35	233.3
95	633.3
140	933.3
220	1466.7

From the above discussions it is clear that MMW-Radar has distinctive advantages over its

lower frequency counterparts. Table 2.5 compares the relative performance of MMW radar with its microwave and optical counterparts for several important radar operating characteristics.

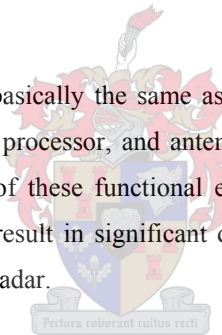
Table 2.5 Radar System Performance Comparison [1].

Radar Characteristics	Microwave	MMW	Optical
Tracking Accuracy	Fair	Fair	Good
Classification or Identification	Poor	Fair	Good
Covertness	Poor	Fair	Good
Volume Search	Good	Fair	Poor
Adverse Weather Performance	Good	Fair	Poor
Performance in Smoke, Dust	Good	Good	Poor

2.4 Fundamental Design Considerations

2.4.1 Functional Elements

The functional elements of MMW radar are basically the same as those of the microwave radar, namely the transmitter, receiver, signal processor, and antenna. Major differences in the operational and performance parameters of these functional elements and the passive components, which connects these elements, result in significant differences in the system level performance of a microwave and MMW radar.



A basic block diagram for typical MMW radar is shown in Figure 2.5. Obviously, a functional radar must include several other components which are linked together, usually by conventional means of connection (cables, printed circuits, etc.) and some form of wave guide, microstrip or MMW integrated circuit techniques.

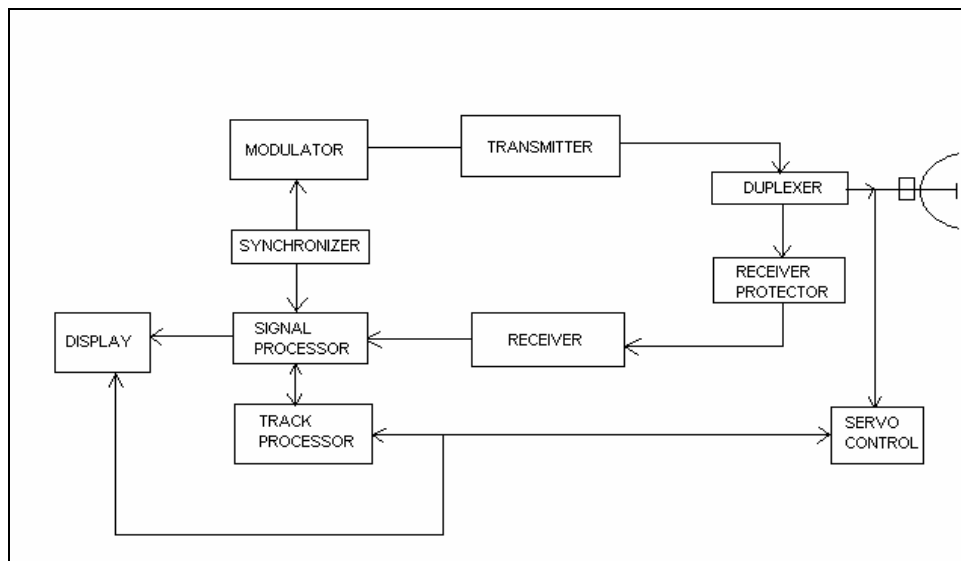


Figure 2.5 Radar block diagram [1].

Some of the most important components include the modulator for timing the basic pulse shaping; a synchronizer to provide system timing; a duplexer to switch the antenna between transmitting and receiving; some form of receiver protection device; a display or interface between the radar and user; antenna servo control; various power supplies; conditioners, and converters.

The following components are essential in MMW-Radar systems:

a) Transmitter

One of the primary performance-determining parameters in any radar design and development is the amount of power available from the radar transmitter and the type of source available. This is particularly true for MMW systems, since they are invariably power limited. The transmitter normally consists of a high-power oscillator, perhaps a magnetron, or a lower power oscillator coupled to a high amplifier such as a Travelling Wave Tube (TWT) or an Extended Interaction Klystron Amplifier (EIKA) [1].

Sources of MMW transmitters can be either solid-state or Thermionic devices. The solid-state sources consist primarily of the IMPATT and Gunn devices. Thermionic sources include magnetrons, Travelling Wave Tubes (TWT), klystrons, EIK oscillators and EIKA, Backward Wave Oscillators (BWO), and gyrotrons.

The performance and accuracy of MMW-Radars is greatly dependant on the performance of the transmitter. This will be discussed in Chapter 3 in more detail.

b) Receiver

The receiver in an MMW radar converts the received signal, collected by the antenna, from a frequency corresponding to the approximate transmitted frequency (depending on Doppler Effects) to a lower or Intermediate Frequency (IF) where it can then be more conveniently filtered, amplified, and processed. The translation of the incoming signal to an IF and the subsequent processing of the lower frequency signal are termed a heterodyne receiver.

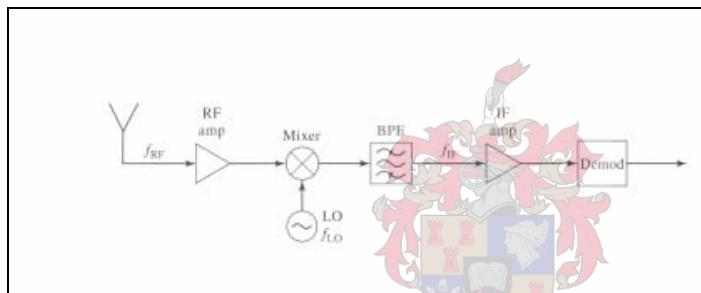


Figure 2.6 Superheterodyne block diagram [4].

A low noise mixer-amplifier combination is normally used to accomplish the down-conversion and first level amplification. This device usually represents the key element of the receiver chain in determining the radar's detection performance, dynamic range, sensitivity, and noise properties [4].

c) Antenna

Most of the antenna technologies and techniques currently in use at MMW involve direct extension of lower frequency approaches. Extended use has been made at MMW of the classic reflector antennas, such as a front-fed parabolic dish and the Cassegrain-fed reflector. A Cassegrain-fed arrangement avoids the waveguide losses associated with the more conventional front-fed reflector which can become excessive at MMW frequencies. Horn and lens (Figure 2.8) antennas are perhaps more popular at MMW than at microwave frequencies. These antennas avoid the aperture blockage and its associated effect on sidelobes common to the reflector antenna. The advantages, when coupled with the advantages of lens antennas over reflector antennas in angle scanning, spill over loss, and fabrication tolerances, makes the lens antenna much more capable of meeting requirements at MMW than lower frequencies. The following figure shows a Cassegrain antenna.



Figure 2.7 Cassegrain antennas [5].



Figure 2.8 Fresnel Lens Mounted in Conical Housing [6].

d) Passive Components

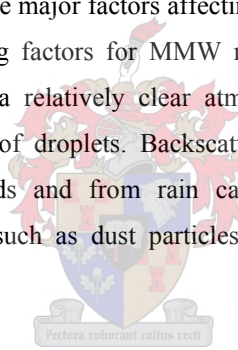
MMW radar requires an array of components which are normally passive to transport, control, attenuate, filter isolators, etc, the MMW energy. These passive components include such devices as waveguide, connectors, couplers, transitions, attenuators, hybrids, filters, circulators, isolators, terminations, matching networks, and duplexers. Many of these devices are simply microwave designs of a particular component scaled up in frequency.

2.4.2 Environment

For radars operating at MMW frequencies, the environment has a significant effect on the overall radar system performance such as target detection range, track accuracy, target discrimination, etc.

a) Attenuation and Reflectivity

Figure 2.9 illustrates in block diagram form the major factors affecting the signal received at any radar. The primary attenuation producing factors for MMW radar are the molecular absorption of water vapour and oxygen in a relatively clear atmosphere, absorption of condensed or suspended water in the form of droplets. Backscatter of energy from the suspended water droplets in fog and clouds and from rain can severely limit radar performance. Suspended particulate matter, such as dust particles and smoke, may also influence MMW propagation.



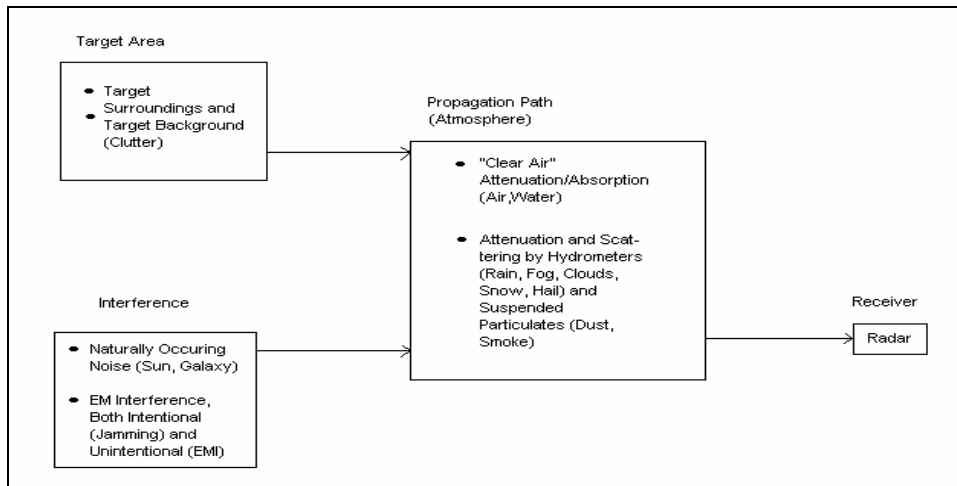


Figure 2.9 Major factors affecting received radar signal [1].

b) Attenuation by Atmospheric Gases, Rain, and Fog

Figure 2.10 shows attenuation produced by basically clear air atmospheric gases at 20°C, one atmospheric pressure, and 7.5g/m³ water vapour [1].

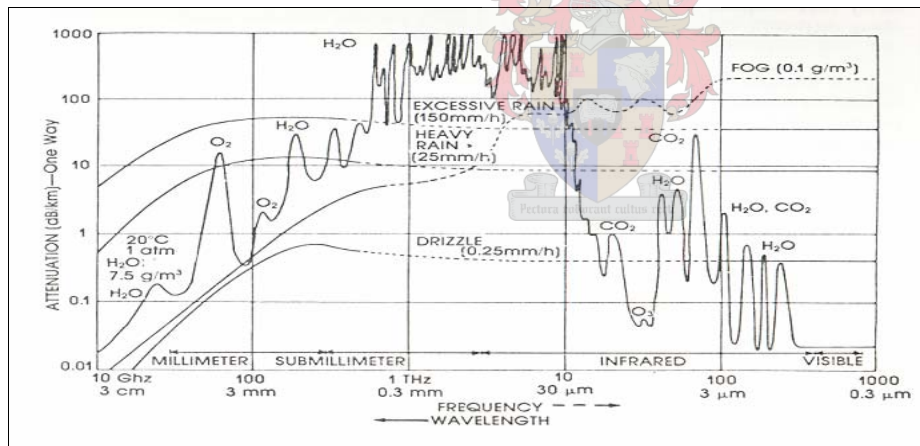


Figure 2.10 MMW and near MMW attenuation by atmospheric gases, rain, and fog [1].

c) Dust, Smoke, and Other Obscurants

One of the primary advantages of MMW sensors over their electro-optical counterparts is enhanced propagation characteristics through dust, smoke, and other battlefield and naturally occurring obscurants.

d) Turbulence Effect

Reflective index inhomogeneities in the propagation path of an MMW signal causes certain propagation phase shifts to result, which in turn result in propagation scintillation effects. Angle of arrival fluctuations are thought to be significant at millimetre wavelengths. Theoretical and experimental investigations of these effects at 94 GHz and 140 GHz have shown that the scintillation effects are not likely to affect MMW systems except at the extreme limits of performance.

e) Multipath Effects

When an RF signal is incident on the surface of the earth, a portion of the incident electromagnetic energy is forward scattered. At the target the energy that reaches the target by the direct path from the transmitter to the target and by reflection from the surface of the earth combines vectorally and can add either in or out of phase. This same phenomenon occurs on the return path from the target to the radar, where it affects tracking accuracy as well as signal strength. Effects produced by these reflected signals, collectively termed “multipath,” can produce fluctuations in signal strength from a target, or in the case of a tracking system, can introduce considerable tracking errors. The magnitude of these multipath related effects is related to an amount of energy incident on the surface, the reflection coefficient of the surface, the amount of energy that reaches the target by the direct path, and the relative phase of the direct and indirect components.

While the analysis of a general multipath situation may be quite complex, considerable insight into the process may be gained by a simplified analysis. In such a simplified analysis, the surface is considered to be a randomly rough surface having known dielectric properties. The voltage reflection coefficient for a smooth surface of the same dielectric material can be calculated, and this modified by a factor to compensate for roughness of the surface in order

to obtain an approximate description of its forward scattering properties. The forward scattering reflection coefficient of a smooth uniform dielectric surface ρ_0 can be calculated directly from the Fresnel equation [1].

The reflection coefficients are then modified by the specular scattering factor, ρ_s where

$$\rho_s^2 = e^{\left[\frac{-(4\pi\sigma_h)\sin\gamma}{\lambda^2} \right]} \quad (2-5)$$

where

σ_h = the rms deviation of the surface height,

λ = wavelength, and

γ = grazing angle.

Note that the surface is considered rough when $\rho_s^2 \leq 0.7$; this is roughly the Rayleigh roughness criterion.

The reflection coefficient for specular reflection is given by

$$\rho = \rho_0 \rho_s \quad (2-6)$$

Equation (2.6) gives the specular reflection coefficient for rough surfaces; there will remain a diffuse component, not as significant in target fading but important in determining tracking error [1].

In general, use of MMW radar may offer the advantage of reduction in multipath effects, primarily because for a given aperture size, the antenna beamwidth decreases with increasing frequency, and since narrow beamwidths can be used to illuminate the target without directing as much energy toward the reflecting earth surface. Also, since roughness is dependant on $\frac{\sigma_h}{\lambda}$ and since λ is small for MMW radars, a given surface appears rougher as

the frequency increases, thus decreasing the specular scattering factor and decreasing ρ .

f) Clutter Characteristics

When a radar system illuminates the earth's surface (land or sea), a portion of the energy is scattered forward, giving rise to multipath effects described above; in addition, a portion of the energy is reflected back toward the radar system. These unwanted signals are usually referred to as "clutter," and can seriously affect overall system performance.

2.4.3 Measures of Performance

MMW radar performance, like its microwave counterpart, is governed by, and can be predicted from, the basic radar range, beacon, and jamming equations. In the case of microwave radars, the atmospheric attenuation term in these equations can usually be neglected, whereas, for MMW radar, it may be the most important factor limiting the radar system's performance.

The performance of a radar system is governed by the complex interrelationship of several system parameters. Analytically, radar performance and trade-off analysis is normally investigated by employing the radar range equation, a mathematical expression that can relate the radar maximum range performance to the complete set of system parameters [1]:

$$R_m^4 = \frac{(P_r G^2 \lambda^2 \sigma 10^{-0.2\alpha R})}{[(4\pi)^3 (kT_0 B) F_n (S/N)_1 L_s]} \quad (2-7)$$

where

R_m^4 = maximum radar range corresponding to the minimum single pulse
signal-to-noise ratio, $(S/N)_1$

$(S/N)_1$ = minimum equivalent receiver output single-pulse signal-to-noise ratio,

P_r = peak radar transmitted power,

λ = radar wavelength,

B = receiver bandwidth $\approx \frac{1}{\tau}$ (for matched receiver), τ is the pulse width,

G = antenna gain,

σ = target cross section,

k = Boltzmann's constant (1.23×10^{23} joule / K),

T_0 = standard reference temperature (290 K),

F_n = receiver noise figure,

α = one-way atmospheric attenuation coefficient, and

L_s = system losses.

As an example of the use of the radar range equation for a simple, first-cut calculation of radar performances, consider the set of postulated radar parameters shown in Table 2.6 for a short range, MMW target acquisition radar. To avoid an iterative solution for determining maximum range (since the propagation loss is range dependent), for convenience a constant loss factor L_T , independent of range is defined which includes both system and atmospheric losses. For this calculation, assume $L_T = 6\text{dB}$. Also, assume no integration or signal processing gain; furthermore, a circular antenna aperture having a gain of 37 dB is assumed.

Table 2.6 Postulated Radar Parameters for Radar Range Calculation [1].

<i>Parameter</i>	<i>Value Assumed</i>
Wavelength λ	3 mm
Transmitter Power P_t	4 kW
Antenna Gain G	37 dB
Pulse Length τ	50 ns
Bandwidth B	20 MHz
Noise Figure F_n	10 dB
Losses L_T	6 dB
Signal-to-Noise (S/N)	13 dB

Using these parameters, the maximum expected radar range is plotted in Figure 2.11.

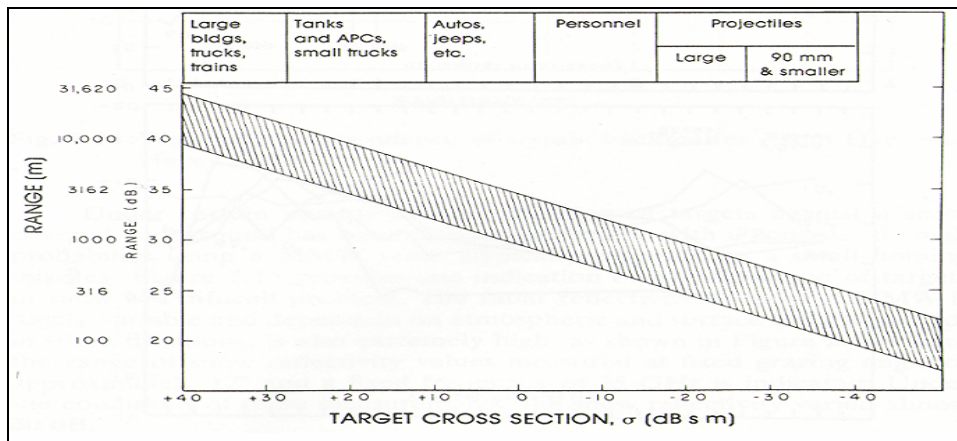


Figure 2.11 Theoretical maximum target detection capabilities of a postulated MMW Radar [1].

2.5 Applications of MMW-Radars

There are a number of applications where MMW radars operating at short-moderate ranges are quite attractive for surveillance and target acquisition. The advantages of millimeter waves for such applications include small size and weight coupled with high resolution in both azimuth and range, providing excellent resolution of the area under surveillance. Table 2.7 gives a summary of the use of MMW radars in the commercial- and military sector.

Table 2.7 Applications of MMW radars in the commercial- and military sectors.

<i>Commercial Sector</i>	<i>Military Sector</i>
MMW radars in the automotive industry	Target acquisition.
MMW radars in the aviation industry.	Missile guidance.
Weather Surveillance.	Battlefield Surveillance.
	MMW radars in the aviation sector.

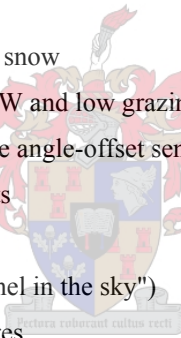
The following section will give examples of some the applications listed in Table 2.7 [5].

2.5.1 Automotive Applications

- Anti collision radar
- Enhanced driving in poor visibility and at night
- Special headlights
- Vision-based guidance of unmanned vehicles
- Road/lane following, lane changing, obstacle detection/avoidance
- Analysis of real-time constraints for vehicle driving
- Vehicle navigation in unknown outdoor environments

2.5.2 Aviation Applications

- Synthetic Vision Systems (SVS) for manual and hands-off landing
- error budgets for SVS-based autoland
- sensors' capabilities in haze, fog, rain, and snow
- characterization of airport surfaces at MMW and low grazing angles
- creation of panoramic views using multiple angle-offset sensors
- electronic windows in windowless cockpits
- line-drawing and photo-realistic displays
- 3D/4D flight guidance displays (e.g., "tunnel in the sky")
- matching of airport/runway/taxiway features
- extraction of vehicle dynamics from image sequences (runway, carrier deck)
- use of SVS measurements in flight-management systems and autopilots
- fully-autonomous computer-vision-based approach and landing
- approach/landing trajectory measurements by computer vision
- simulation of weather conditions and SVSs in flight simulators
- Synthetic Vision (SV) for helicopters and tilt-rotor aircraft (including wire detection)
- SV for landing on aircraft/helicopter carriers
- SV for hypersonic transports, e.g., in High Speed Research (HSR) program



- SV for Unmanned Air Vehicles (UAVs)
- SV for runway and taxiway following, obstacle detection (e.g., runway incursions)
- night vision, including "colour night vision"
- detection of dangerous weather (microbursts, windshears, etc.)
- combining of SV and weather radar
- other vision-based Enhanced Situation Awareness Systems (ESAS)

2.6 Characteristics of basic components

To gain a better understanding of the existing system a closer look at the characteristics of the components is needed. The following block diagram shows the basic components of the existing MMW-Radar.

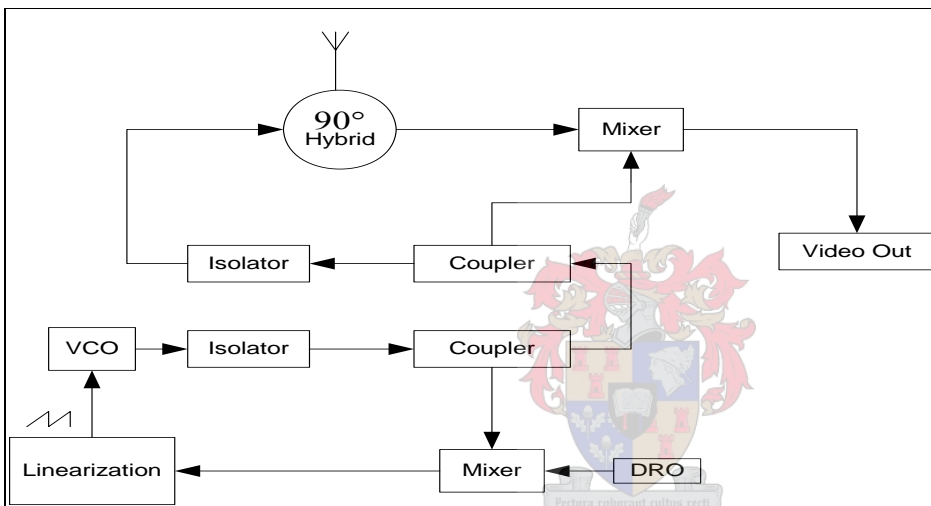


Figure 2.12 Block diagram of MMW-Radar.

The following section introduces the components of Figure 2.12 and describes the characteristics of each component.

2.6.1 Antenna

The performance and accuracy of the MMW-Radar are greatly dependent on the performance of the antenna. The antenna characteristics plays a big role in the resolution and range of the system. As mentioned in the previous section, extended use has been made at MMW of the classic reflector antenna. This specific radar uses a parabolic dish antenna shown in Figure 2.13. Table 2.8 gives the specification of this particular antenna.

Table 2.8 Parabolic dish antenna specifications [6].

Test Frequency	94 GHz
3.0 dB Beamwidth in the E-plane	0.95 degrees
3.0 dB Beamwidth in the H-plane	0.85 degrees
1 st sidelobe suppression in the E-plane	21.7 dB
1 st sidelobe suppression in the H-plane	21.0 dB
Gain	45.5 dB



Figure 2.13 Photo Taken of Parabolic dish antenna.

Figure 2.14 and Figure 2.15 shows the radiation pattern in the E-plane and H-plane of the parabolic dish antenna.

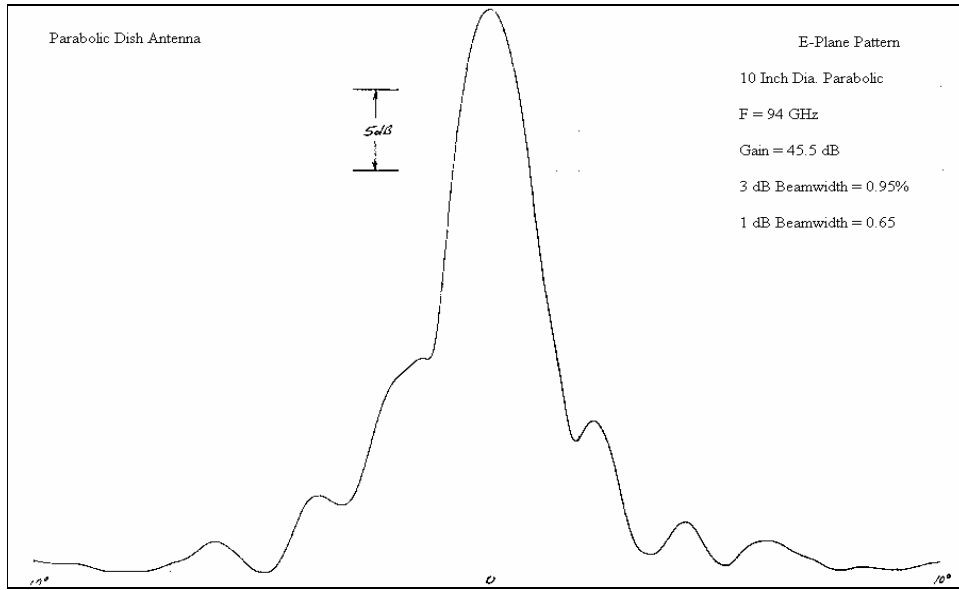


Figure 2.14 E-Plane radiation pattern of antenna [6].

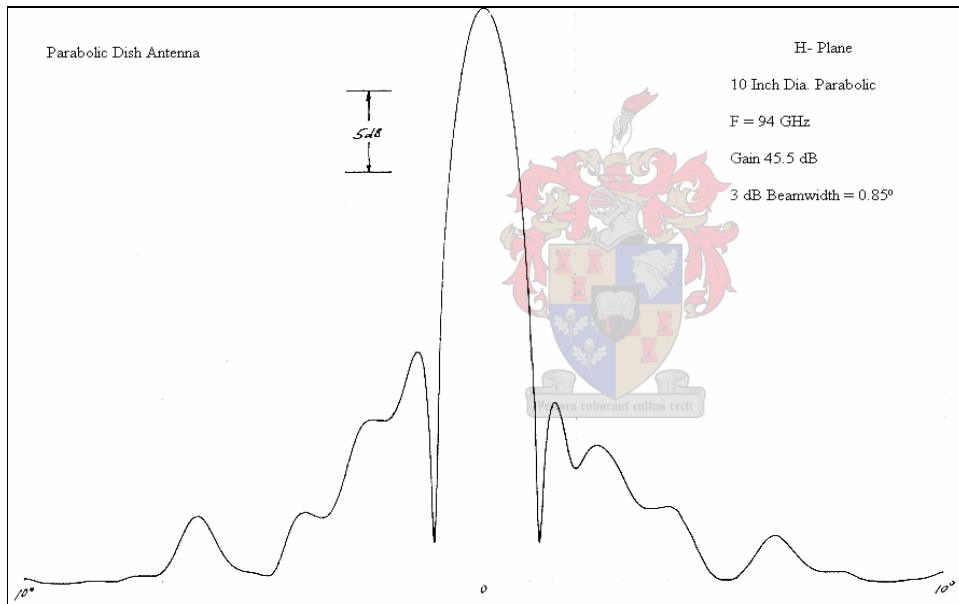


Figure 2.15 H-Plane radiation pattern of antenna [6].

2.6.2 Quadrature (90°) Hybrid

Quadrature hybrids are 3 dB directional couplers with 90° phase difference in the outputs of the through and coupled arms [4]. The hybrid makes it possible to use one antenna for transmitting and receiving. Figure 2.16 shows an example of a quadrature hybrid

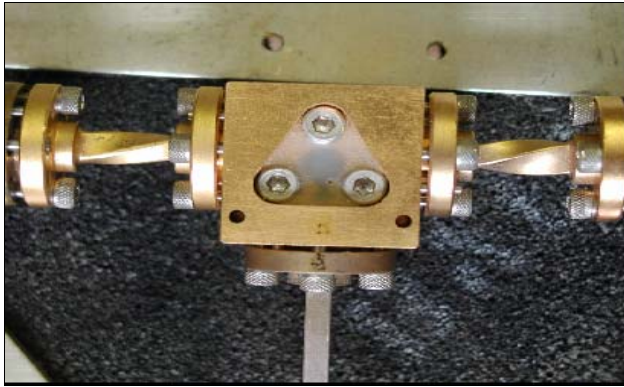


Figure 2.16 Photo taken of Quadrature Hybrid.

Table 2.9 shows typical characteristics of a quadrature hybrid.

Table 2.9 Typical characteristics of a quadrature hybrid [7]

Frequency Range	75 – 106 GHz
Amplitude Imbalance	+/- 0.5 dB
Phase Imbalance	+/- 10 degrees
<u>Isolation (Min):</u>	
H-Arm Port	30 dB
E-Arm Port	20 dB
<u>VSWR (Max):</u>	
H-Arm Port	1:5:1
E-Arm Port	1:6:1
Insertion Loss (Max)	1 dB

2.6.3 Coupler

The couplers are used to supply reference frequencies to the various mixers of the system.

Figure 2.17 shows an example of typical coupler used in MMW systems.



Figure 2.17 Photo taken of Millitech coupler.

Table 2.10 Table 2.10 shows typical characteristics of an MMW coupler.

Table 2.10 Measured characteristics of Millitech coupler [8].

Frequency band	75-110 GHz
Coupling value	10.49 dB at 92.5 GHz
Coupling flatness	0.42 dB
Insertion loss	1.2 dB
Directivity	24 dB
Main line VSWR (max) [12]	1.10:1
Secondary line VSWR (max) [12]	1.15:1

2.6.4 Dielectric Resonator Oscillator (DRO)

The 94.5 GHz frequency of the VCO needs to be mixed down to a lower workable frequency. This is done by using an X-band (13.5 GHz) DRO shown in Figure 2.18. The DRO is a very stable oscillator and would be ideal to use as a reference frequency for the harmonic mixer.

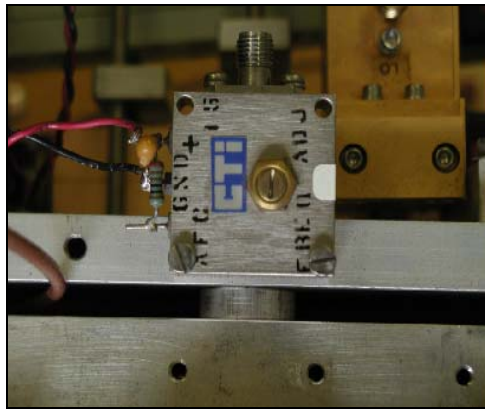


Figure 2.18 Photo taken of CTI Dielectric Resonator Oscillator.

Table 2.11 gives typical characteristics of a DRO.

Table 2.11 Measured characteristics of CTI DRO [9].

RF Frequency Range	13500 MHz
RF Power Output (Across Band): Min.	5.60 dBm
Max.	6.00 dBm
Spurious Output: In Band	-80 dBc
Out-of-Band	-80 dBc
Harmonics	-20 dBc
Phase Noise: @10 kHz	-75 dBc/Hz
@ 100 kHz	-105 dBc/Hz
Supply Voltage	+15 V
Supply Current	54.4 mA
Δ Frequency	± 15 MHz min.

2.6.5 Harmonic Mixer

A mixer is used to convert the high transmitted frequency down to a lower frequency. This is necessary because a lot of the components in the system work at a much lower frequency than the transmitted frequency. Different types of mixers are available. For this application a harmonic mixer shown in Figure 2.19 is used to mix the 94.5 GHz VCO frequency down to a lower frequency. This is done by using the stable DRO described in the previous section. The mixer uses the n^{th} harmonic of the DRO as an input to produce an IF of 10 – 2000 MHz.



Figure 2.19 Photo taken of Harmonic Mixer.

Table 2.12 gives the typical characteristics of a harmonic mixer.

Table 2.12 Measured characteristics of Harmonic Mixer [10].

RF Bandwidth	75 – 110 GHz
LO Signal	94 GHz
IF Bandwidth	10 – 2000 MHz
RF Power	-10 dBm
LO Power	0 dBm
Conversion Loss	± 25 dBm
LO–RF Isolation	18 dB
IF Power	- 45 dBm

2.6.6 Isolator

The system is very sensitive to return signals. The isolator is used to protect the transmitter from any return signals. The following figure shows an isolator supplied by Terabeam.



Figure 2.20 Isolator supplied by Terabeam [11].

Table 2.13 gives typical characteristics of an isolator.

Table 2.13 Typical characteristics of MMW isolators [11].

Frequency Band	92 – 95 GHz
Input/Output VSWR	1.3:1 (max)
Insertion Loss	0.6 dB (max)
Isolation	22.5 dB (min)

2.6.7 Voltage Controlled Oscillator (VCO)

In a CWFM Radar system the detection of a target will result in the transmitted signal to be shifted in time. The range of the target will therefore be equal to the difference between the transmitted and received signal. This difference is measured by coupling the transmitted signal to the mixer to be used as the reference signal to mix the received signal down to produce the IF, shown in Figure 2.12. This is one of the reasons why the VCO is one of the most important components of the system. The resolution and accuracy of target detection will be directly dependant on the performance and linearity of the VCO. A typical MMW VCO is shown in Figure 2.21.



Figure 2.21 Gunn VCO supplied by Millitech [12].

It is important to characterize the VCO in order to improve the linearity of the system.

Table 2.14 gives typical characteristics of an MMW VCO.

Table 2.14 Measured characteristics of Millitech VCO.

Centre Frequency	94 GHz
Varactor Tuning Range	+/-500 MHz
Power Output	20 mW
Gunn Diode Bias Voltage	10.3 V
Gunn Diode Operating Current	220 mA
Maximum Operating Voltage	10.5 V
Varactor Voltage	0 to +9V
Typical Frequency Stability [14]	-5 MHz/°C
Typical Power Stability [14]	-0.04 dB/°C

Figure 2.22 shows the measured output power of the VCO over its frequency tuning range

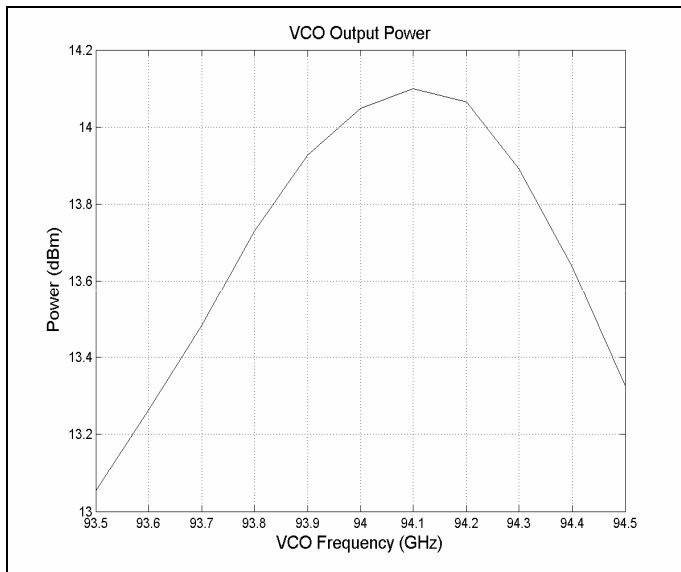
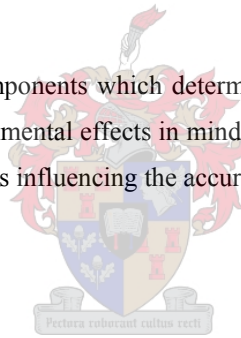


Figure 2.22 Measured VCO Output power.

2.7 Conclusion

The antenna and VCO are the two major components which determine the performance of MMW systems. It is important to keep environmental effects in mind when designing MMW systems. The next chapter introduces the factors influencing the accuracy of MMW systems.



3 Factors influencing the accuracy of the system

This chapter introduces the radar range equation and Doppler effect for pulse and CW-radars. It is necessary to understand these concepts before looking at the effects that the modulation and deviation frequencies have on the linearity of the system. The effects of the modulation and deviation frequencies are simulated using Matlab [19] in the frequency and time domain to give insight to the effects of the modulation and deviation frequency in the system.

3.1 The Doppler Effect

A radar detects the presence of objects and locates their position in space by transmitting electromagnetic energy and observing the returned echo. A pulse radar transmits a relatively short burst of electromagnetic energy, after which the receiver is turned on to listen for the echo. The echo not only indicates the presence of a target, but the time that elapses between the transmission of the pulse and the receipt of the echo is a measure of the distance to the target. Separation of the echo signal and the transmitted signal is made on the basis of difference in time.

The radar transmitter may be operated continuously rather than pulsed if the strong transmitted signal can be separated from the weak echo. The receiver-echo-signal power is considerably smaller than the transmitted power; it may be as little as 10^{-18} that of the transmitted power – sometimes even less. Separate antennae for transmission and reception help segregate the weak echo from the strong leakage signal, but isolation is usually not sufficient. A feasible technique for separating the received signal from the transmitted signal when there is relative motion between radar and target is based on recognising the change in the echo-signal frequency caused by the doppler effect [2].

It is well known in the field of optics and acoustics that if either the source of oscillation or the observer of the oscillation is in motion, an apparent shift in frequency will result. This is the doppler effect and is the basis of the CW radar. If R is the distance from the radar to the target, the total number of wavelengths λ contained in the two-way path between the radar

and the target is $\frac{2R}{\lambda}$. The distance R and the wavelength λ are assumed to be measured in the same units. Since one wavelength corresponds to an angular excursion of 2π radians, the total angular excursion ϕ made by the electromagnetic wave during its transit to and from the target is $\frac{4\pi R}{\lambda}$ radians. If the target is in motion, R and the phase ϕ are continually changing. A change in ϕ with respect to time is equal to a frequency. This is the doppler angular frequency ω_d , given by [2]

$$\omega_d = 2\pi f_d = \frac{d\phi}{dt} = \frac{4\pi}{\lambda} \frac{dR}{dt} = \frac{4\pi v_r}{\lambda} \quad (3-1)$$

Where f_d = doppler frequency shift and v_r = relative (or radial) velocity of target with respect to radar. The doppler frequency shift is

$$f_d = \frac{2v_r}{\lambda} = \frac{2v_r f_o}{c} \quad (3-2)$$

where f_o = transmitted frequency and c = velocity of propagation = 3×10^8 m/s.

The relative velocity may be written $v_r = v \cos \theta$, where v is the target speed and θ is the angle made by the target trajectory and the line joining radar and target.

The CW radar is of interest not only because of its many applications, but its study also serves as a means for better understanding the nature and use of the doppler information contained in the echo signal. In addition to allowing the received signal to be separated from the transmitted signal, the CW radar provides a measurement of relative velocity which may be used to distinguish moving targets from stationary objects or clutter.

3.2 CW Radar

Consider the simple CW radar as illustrated by the block diagram of Figure 3.1. The transmitter generates a continuous (unmodulated) oscillation of frequency f_o , which is

radiated by the antenna. A portion of the radiated energy is intercepted by the target and is scattered, some of it in the direction of the radar, where it is collected by the receiving antenna. If the target is in motion with a velocity v_r relative to the radar, the received signal will be shifted in frequency from the transmitted frequency f_0 by an amount $\pm f_d$ as given by equation

$$f_d = \frac{2v_r}{\lambda} = \frac{2v_r f_0}{c} \quad (3-2)$$

The plus sign indicates a target moving towards the radar and the minus sign indicates a target moving away from the radar. The received echo signal at a frequency $f_0 \pm f_d$ enters the radar via the antenna and is heterodyned in the detector (mixer) with a portion of the transmitted signal f_0 to produce a doppler beat note of frequency f_d . The sign of f_d is lost in the process.

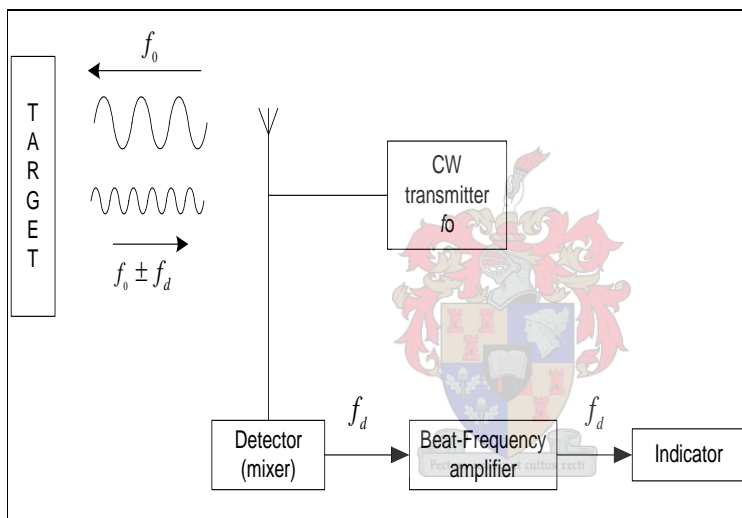


Figure 3.1 Simple CW radar block diagram [2].

The inability of the simple CW radar to measure range is related to the relatively narrow spectrum (bandwidth) of its transmitted waveform. Some sort of timing mark must be applied to a CW carrier if range is to be measured. The timing mark permits the time of transmission and the time of return to be recognized. The sharper or more distinct the timing mark, the

more accurate the measurement of transit time. But the more distinct the timing mark, the broader the transmitted spectrum. This allows from the properties of the Fourier transform. Therefore a finite spectrum must of necessity be transmitted if transit time or range is to be measured.

The spectrum of a CW transmission can be broadened by application of modulation, either amplitude, frequency, or phase.

3.3 Frequency-Modulated CW Radar

A widely used technique to broaden the spectrum of CW radar is to frequency-modulate the carrier. The timing mark is the changing frequency. The transit time is proportional to the difference in frequency between the echo signal and the transmitter signal. The greater the transmitter frequency deviation in a given time interval, the more accurate the measurement of the transit time and the greater the transmitted spectrum.

3.4 Range and doppler measurement

In the FM-CW radar the transmitter frequency is changed as a function of time in a known manner. Assume that the transmitter frequency increases linear with time, as shown by the solid line in Figure 3.2.

If there is a reflecting object at a distance R, an echo signal will return after a time, T. The distance of the target can then be calculated using the next equation [2].

$$T = \frac{2R}{c} \quad (3-3)$$

The dashed line in the Figure 3.2 represents the echo signal. If the echo signal is heterodyned with a portion of the transmitter signal in a nonlinear element such as a diode, beat note f_b will be produced. If there is no doppler frequency shift, the beat note is a measure of the target's range and $f_b = f_r$, where f_r is the beat frequency due only to the target's range. If the rate of change of the carrier frequency is \dot{f}_0 , the beat frequency is [2]

$$f_r = f_0 T = \frac{2R}{c} f_0 \quad (3-4)$$

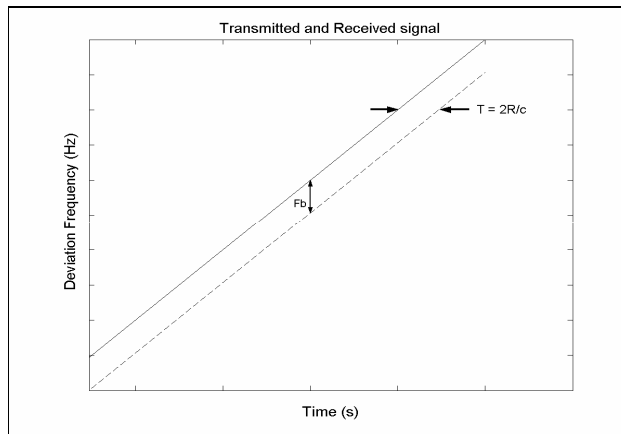


Figure 3.2 Linear frequency modulation [2].

In any practical CW radar, the frequency cannot be continually changed in one direction only. Periodicity in the modulation is necessary, as in the triangular frequency-modulation waveform shown in Figure 3.3.

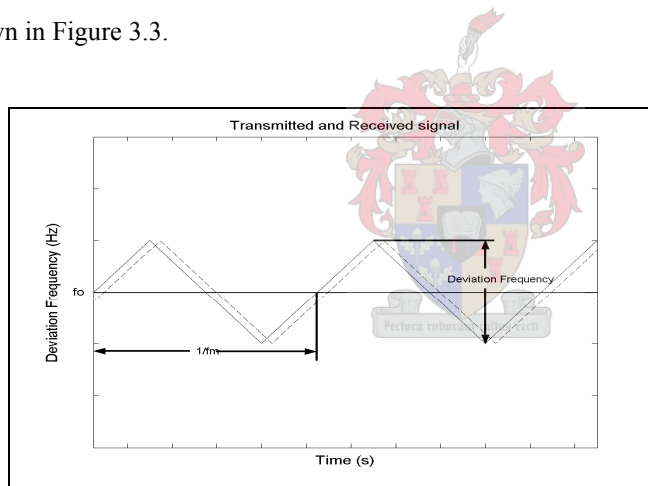


Figure 3.3 Triangular Frequency Modulation [2].

The resulting beat frequency as a function of time is shown in Figure 3.4 for triangular modulation.

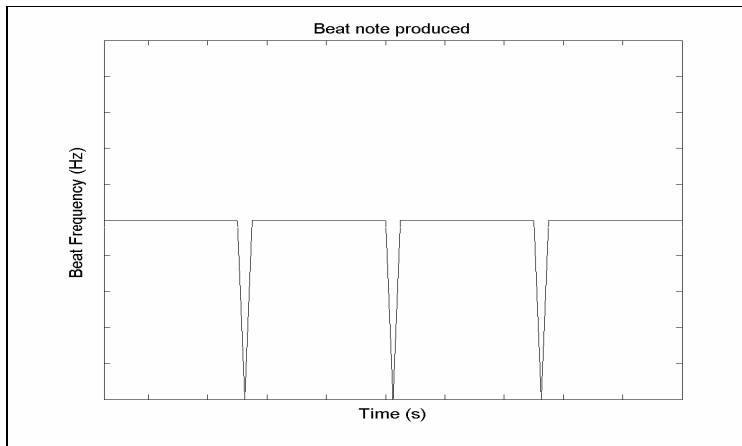


Figure 3.4 Beat note produced from target range [2].

The beat note is of constant frequency except at the turn-around region. If the frequency is modulated at a rate f_m over a range Δf , the beat frequency is

$$f_r = \frac{2R}{c} 2\dot{f}_m = \frac{4Rf_m\Delta f}{c} \quad (3-5)$$

Thus the measurement of the beat frequency determines the range R.

In the above, the target was assumed to be stationary. If this assumption is not applicable, a doppler frequency shift will be superimposed on the FM range beat note and an erroneous range measurement results. The doppler frequency shift causes the frequency-time plot of the echo signal to be shifted up or down. On one portion of the frequency-modulation cycle, the beat frequency is increased by the doppler shift, while on the other portion, it is decreasing as shown in

. If, for example, the target is approaching the radar, the beat frequency $f_b(up)$ produced during the increasing portion of the FM cycle will be the difference between the beat frequency due to the range f_r and the doppler frequency shift f_d equation (3-6). Similarly, on the decreasing portion, the beat frequency $f_b(down)$ is the sum of the two equations [2] (3-7).

$$f_b(up) = f_r - f_d \quad (3-6)$$

$$f_b(\text{down}) = f_r + f_d \quad (3-7)$$

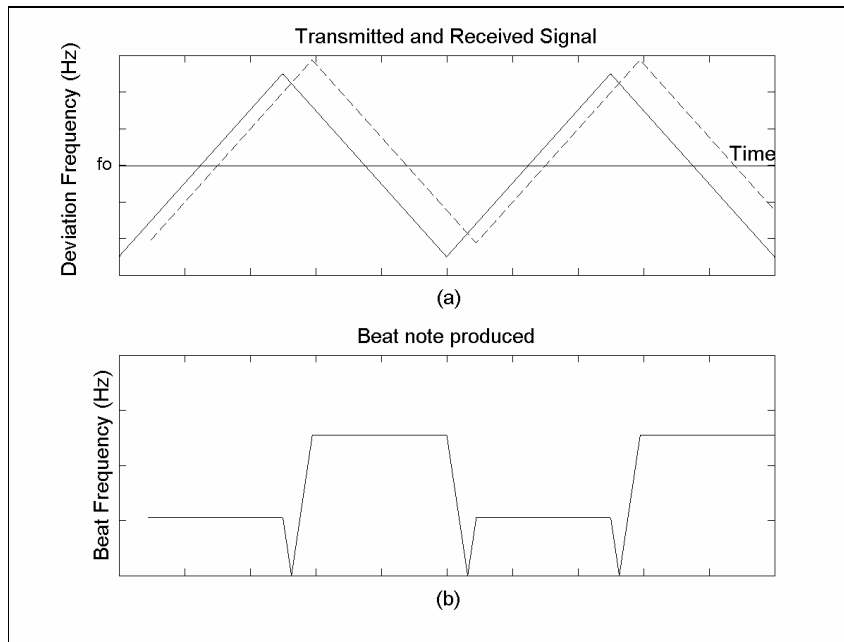


Figure 3.5 Frequency-time relationship in FM - CW radar when received signal is shifted by the doppler effect (a) Transmitted (solid curve) and echo (dashed line) frequencies; (b) beat frequency [2].

The range frequency f_r may be extracted by measuring the average beat frequency; that is, $\frac{1}{2}[f_b(\text{up}) + f_b(\text{down})] = f_r$. If $f_b(\text{up})$ and $f_b(\text{down})$ are measured separately. For example, by switching a frequency counter every half modulation cycle, one-half the difference between the frequencies will yield the doppler frequency. This assumes $f_r > f_d$. If, on the other hand, $f_r < f_d$, such as might occur with a high-speed target at short range, the roles of the averaging and the difference-frequency measurements are reversed; the averaging meter will measure doppler velocity, and the difference meter, range. If it is not

known that the roles of the meter are reversed because of a change in the inequality sign between f_r and f_d , an incorrect interpretation of the measurements may result.

If the motion of the targets were to produce a doppler shift, or if the frequency-modulation waveform were nonlinear, or if the mixer were not operated in its linear region, the problem of resolving the targets and measuring the range of each becomes more complicated.

3.4.1 Modulation Frequency

The modulation frequency, f_m , is the rate at which the transmitted signal's frequency is changed around its centre frequency, f_0 . Two popular modulation waveforms are the saw tooth modulation shown in Figure 3.6 and the triangular modulation shown in Figure 3.7. For this application the triangular modulation is used.

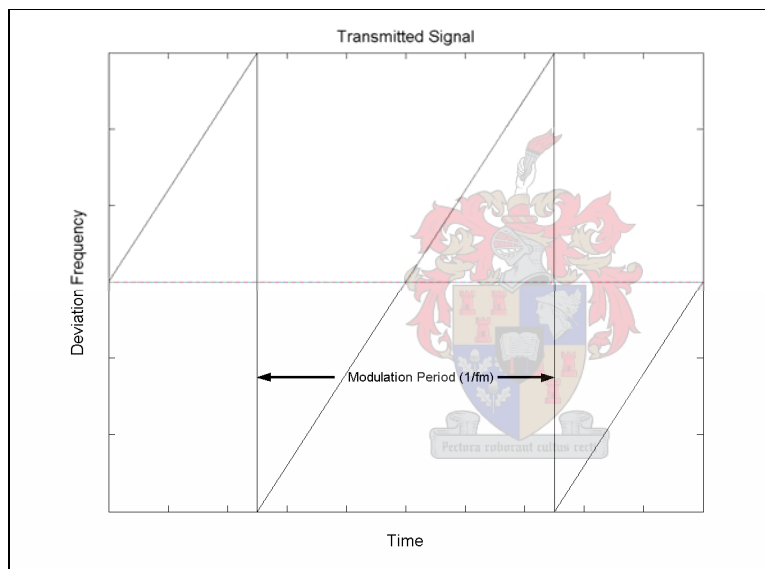


Figure 3.6 Simulation of saw tooth frequency modulation [19].

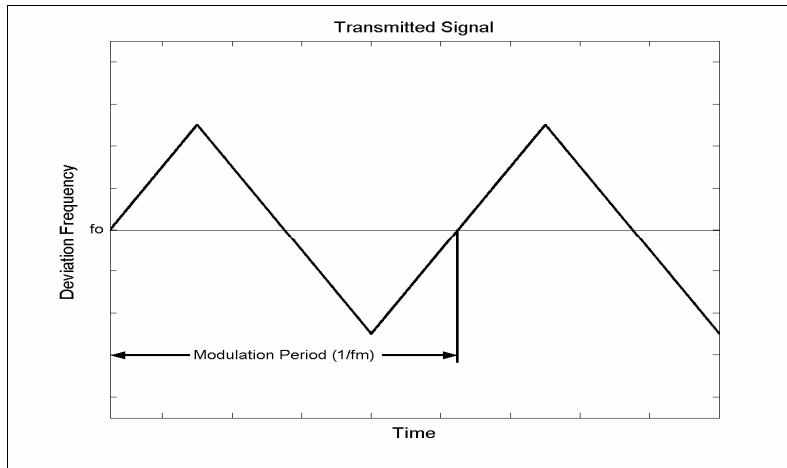


Figure 3.7 Simulation of triangular frequency modulation [19].

The modulation frequency will determine the maximum unambiguous range of the radar. The delay time of the echoed signal determines the range of the target equation (3-3). This delay time cannot be greater than half the modulation period. This effect is illustrated in the following figures.

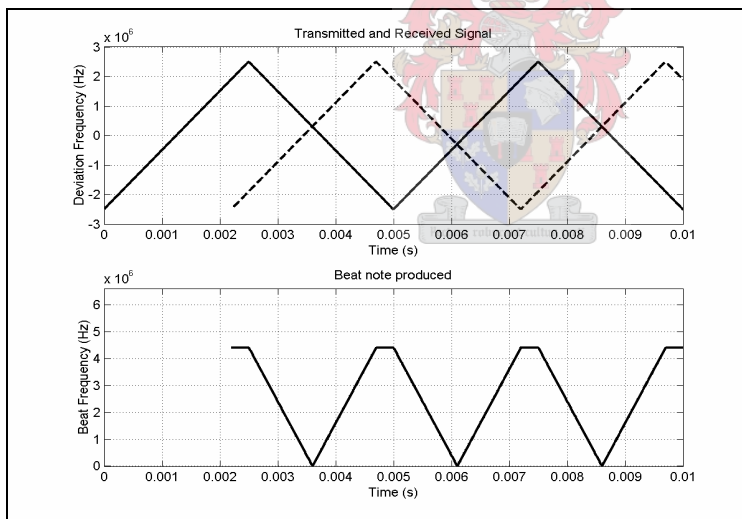


Figure 3.8 Unambiguous beat note [2].

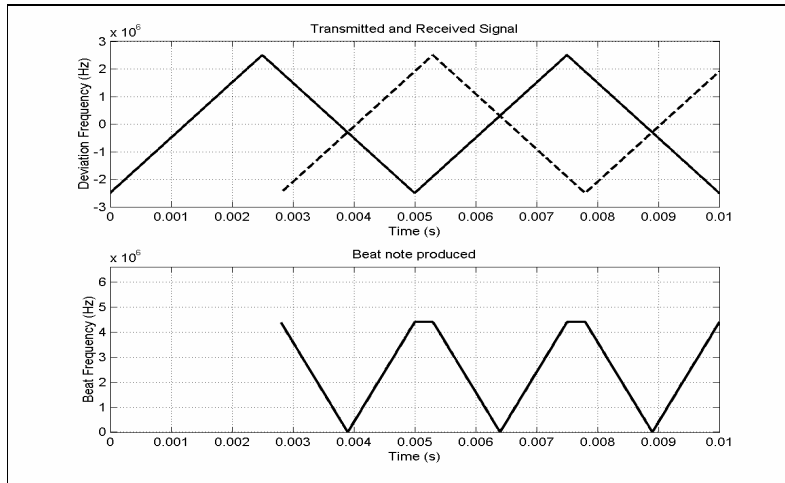
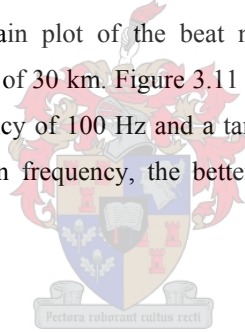


Figure 3.9 Ambiguous beat note [2].

As indicated by Figure 3.8 and Figure 3.9, the same beat note is produced for targets at different distances. It will then be impossible to determine the correct distance of the target. The modulation frequency will also have an effect on the resolution of the beat note produced. Figure 3.10 shows the time domain plot of the beat note, for a modulation frequency of 500 Hz and a target at a distance of 30 km. Figure 3.11 shows the time domain plot of the beat note for a modulation frequency of 100 Hz and a target at a distance of 30 km. It is clear that the lower the modulation frequency, the better the resolution of the system.



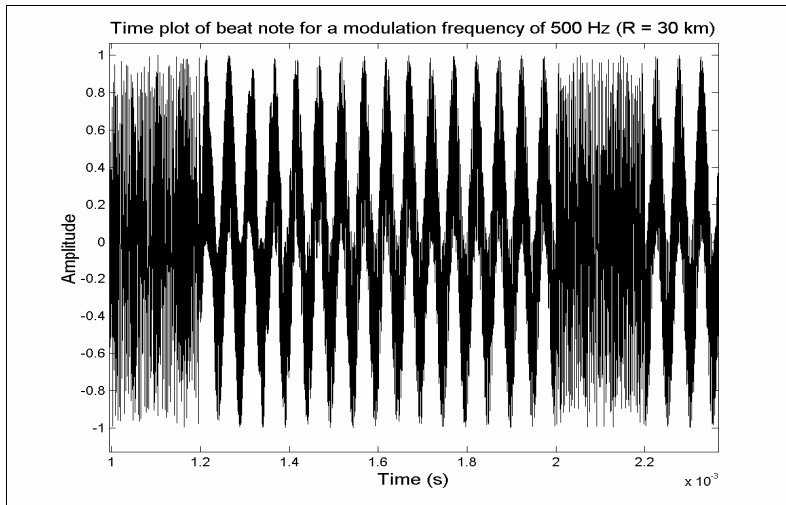


Figure 3.10 Time domain simulation of beat note for a modulation frequency of 500 Hz [19].

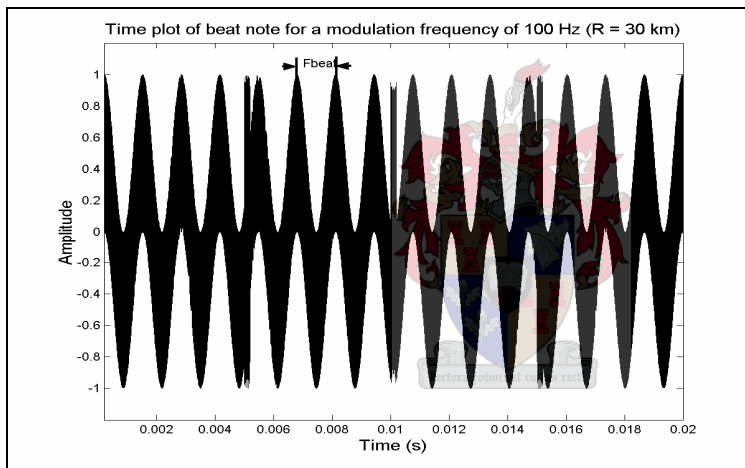


Figure 3.11 Time domain simulation of beat note for a modulation frequency of 100 Hz [19].

3.4.2 Deviation Frequency

Another parameter that the radar designer can change is the deviation frequency. The deviation frequency is the magnitude of change in centre frequency of the transmitted signal. The resolution of the beat note produced is also affected by the choice of the deviation frequency. Figure 3.12 illustrates a beat note produced from a target at a distance of 30 km and a deviation frequency of 500 MHz.

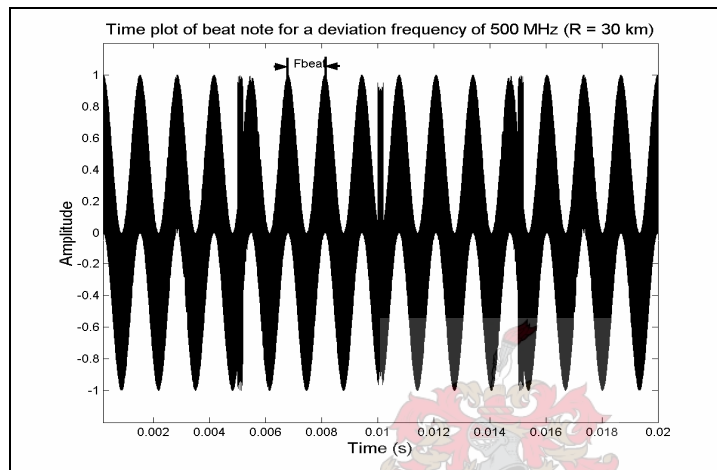


Figure 3.12 Time domain simulation of deviation frequency of 500 MHz [19].

Figure 3.13 illustrates a beat note produced from the same target, but with a deviation frequency of 50 MHz.

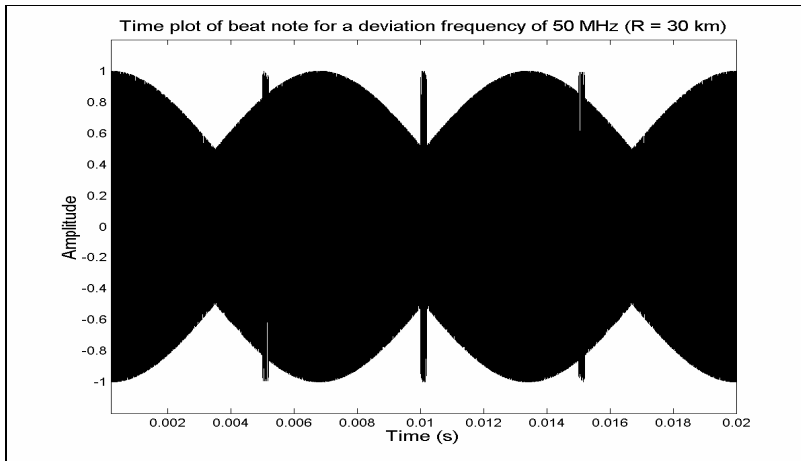


Figure 3.13 Time domain simulation of deviation frequency of 50 MHz [19].

From Figure 3.13, it is clear that for a higher deviation frequency, the higher the resolution of the beat note produced would be. It is clear from the above discussion that the modulation and deviation frequencies are important design considerations in determining the resolution and performance of radars.

3.5 Linearity of the transmitted signal

If the modulation frequency changes linearly with time, the beat note produced by a target at a distance R from the radar, will be constant. The following figure illustrates this.



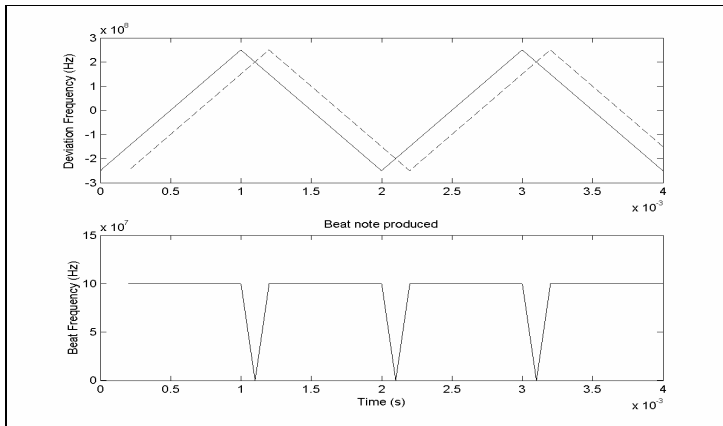


Figure 3.14 Simulation of linear modulation [19].

The dashed line in Figure 3.14 represents the echoed signal. If the modulation is not linear, the beat note produced will not be constant any more. If there is only one target present, the distance can still be determined by measuring the average beat frequency over a modulation cycle. This method requires advanced and complicated signal processing, and it would therefore be better if the modulation frequency can be linear. Figure 3.15 shows the effect if the modulation is not linear.

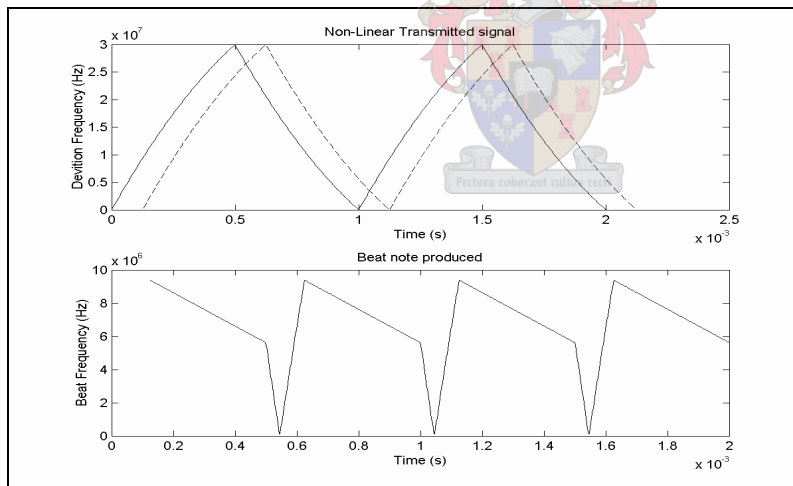


Figure 3.15 Simulation of nonlinear modulation [19].

The following sections will deal on the influence of nonlinear modulation in the time- and frequency domain.

3.5.1 Influence of nonlinear modulation in the time domain

The influence of nonlinear modulation in the time domain is simulated in Matlab and illustrated in Figure 3.16.

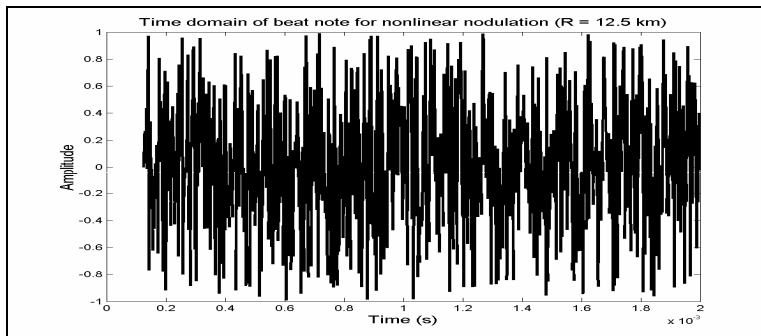


Figure 3.16 Time domain simulation of nonlinear modulation [19].

From Figure 3.16 it is clear that it will be impossible to determine the beat frequency without any additional signal processing.

3.5.2 Influence of nonlinear modulation in the frequency domain

The following figure shows the influence of nonlinear modulation in the frequency domain.

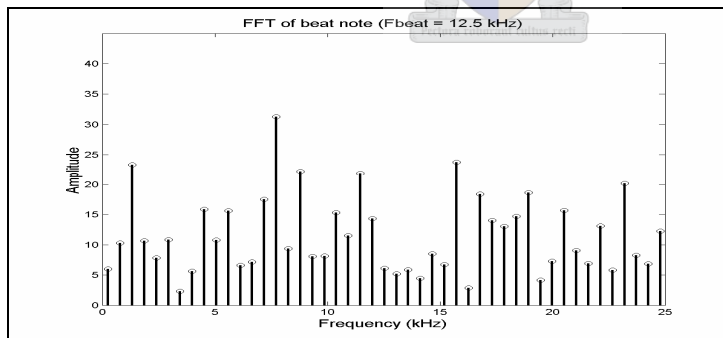


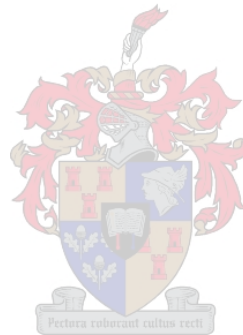
Figure 3.17 Simulated FFT of beat note for nonlinear modulation [19].

From Figure 3.17 it is clear that additional signal processing will be necessary if the beat frequency is to be acquired.

3.6 Conclusion

Linearity of the modulation frequency is critical to ensure accurate range measurements. Nominal linearity of 1 % in the radar front end translates directly to the equivalent range accuracy. This implies that a range error introduced by the radar at 250 metres will nominally be 2.5 metres. MMW applications are specifically chosen for the excellent resolution obtained.

Nonlinearity of the modulation frequency is a direct result of the characteristics of the transmitter. Factors such as frequency drift, temperature effects, nonlinearity in output frequency vs. tuning voltages, and phase noise are critical in determining the linearity of the modulation frequency. The next chapter introduces linearization techniques concentrating only on the linearization of the modulation frequency supplied by the VCO.



4 Linearization Techniques

This chapter introduces the various linearization techniques with an in depth study on the closed loop linearization technique. The advantages and disadvantages of the techniques are discussed and compared.

4.1 Definition of VCO linearization techniques

Linearity is defined by,

$$L = \frac{\text{Slope}_{\max} - \text{Slope}_{\min}}{\text{Slope}_{\min}} \quad (4-1)$$

The linearity of the 94.5 GHz VCO was measured and calculated to be in the region of 3 % over a 1 GHz bandwidth. The following graph shows the measured output frequency of the VCO.

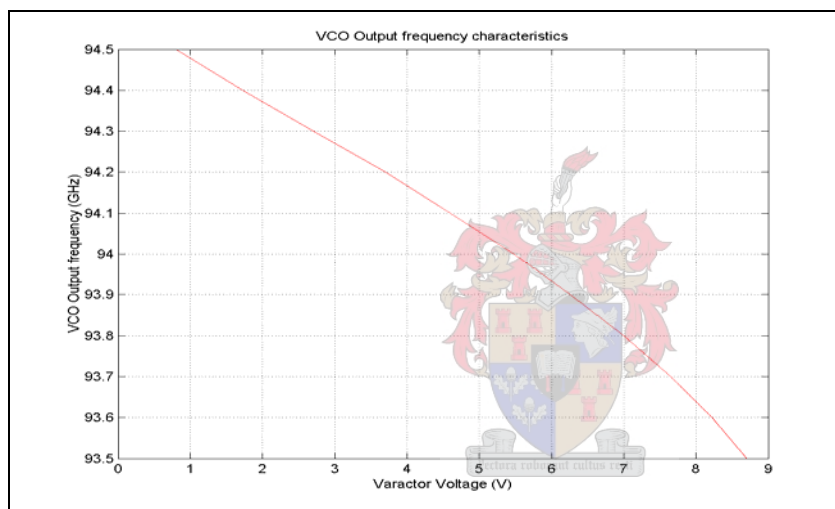


Figure 4.1 Measured VCO output frequency.

Possible techniques to improve the linearity of the VCO will be discussed in the following section. They are:

1. Open loop linearization
2. Closed loop linearization technique using a frequency discriminator

3. Phase Lock Loop linearization technique using a direct synthesizer

4.2 Open Loop Linearization Technique

Open loop linearization is a relatively inexpensive and easy technique to use. The desired linearity can be obtained by accurately characterizing the VCO output frequency for all environmental conditions [13]. The open loop linearization is then performed by adjusting the input tuning voltage of the VCO to compensate for the non-linearity of the VCO output frequency shown in Figure 4.2. This is normally implemented by using look up tables to adjust the input for different environmental states. This method is only suitable if the VCO is operated at a constant temperature.

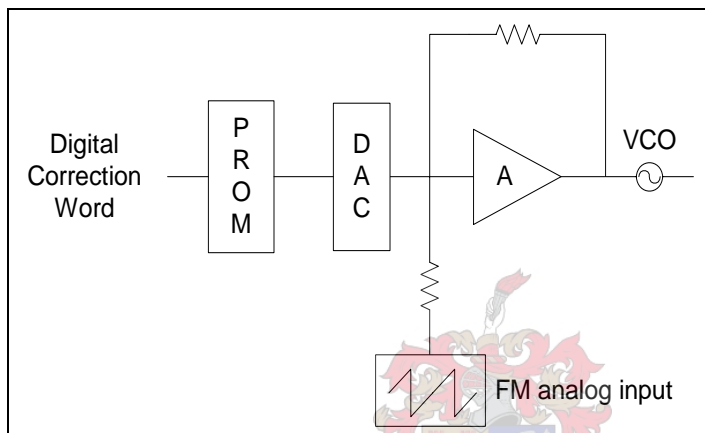


Figure 4.2 Open loop diagram [13].

It will be impossible to characterize the VCO output frequency for every single environmental condition. This means that the VCO output frequency will not stay linear for unpredicted changes in the environment. The VCO will also experience frequency drift because of thermal effects. The open loop linearization technique will not be able to compensate for these frequency drifts. Open loop linearization does not improve the noise characteristics of the VCO.

The open loop linearization technique is therefore not suitable for systems where a high level of accuracy is required.

4.3 Closed loop linearization technique using a frequency discriminator

To overcome the problem discussed in the previous section, the VCO must be placed in a closed feedback loop to ensure that the environmental changes will have no effect on the output frequency of the VCO [13].

Figure 4.3 shows a closed loop linearization technique with a frequency discriminator (FD) in the feedback loop. The operating frequency of the components used in the loop are lower than that of the VCO output frequency. It is therefore necessary to mix and divide the VCO frequency down which does not change the linearity requirements of the FD. The mixing and dividing does have an influence on the bandwidth of the loop.

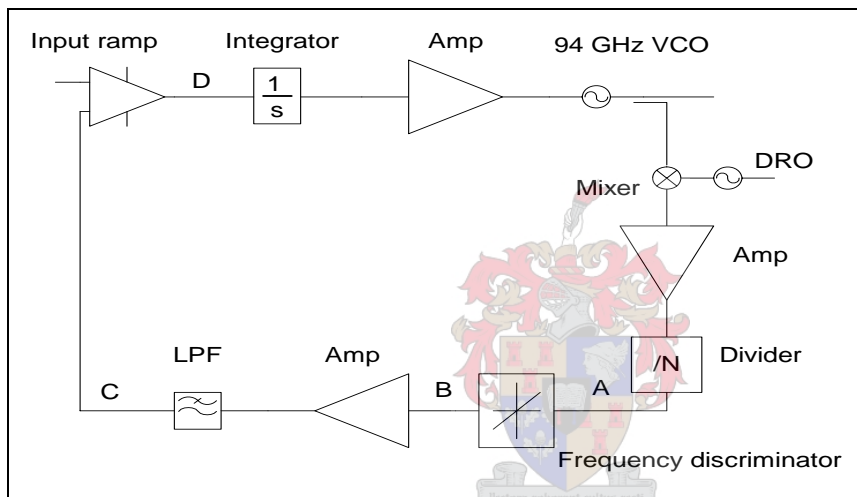


Figure 4.3 Frequency discriminator in feedback loop [13].

A frequency discriminator converts frequency changes into amplitude changes; or in other words, an FM to AM converter as shown in Figure 4.4. The VCO output signal is coupled to be the reference of the FD. The VCO follows the characteristic frequency-voltage curve of the frequency discriminator. The improvement in linearity will therefore be dependant on the performance of the FD.

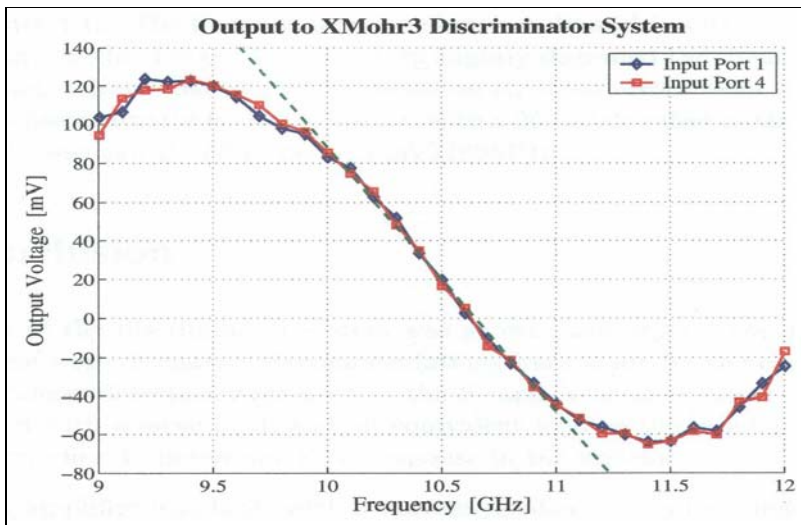


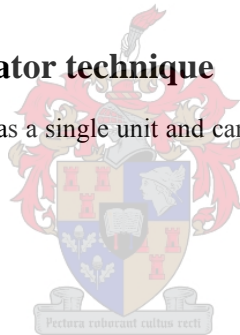
Figure 4.4 Typical voltage-frequency response of a frequency discriminator [14].

The following section will give examples of different frequency discriminators that can be used in a closed feedback loop.

4.3.1 Digital frequency discriminator technique

Digital frequency discriminators are available as a single unit and can be used directly in the feedback loop. Key specifications are [13]:

- resolution (e.g. 8-bits)
- measurement speed
- bandwidth
- voltage-frequency response.



To understand the feedback loop, it is necessary to look at the signal at different points in the loop shown in Figure 4.3.

Point A: At this point the frequency of the VCO is already mixed down and divided by N . The division is necessary to reduce the sweep bandwidth of the VCO to be within the limits

of the FD. The division factor N has an influence on the VCO noise floor. The noise floor increases with a factor $20 \log_{10} N$ (dBc/Hz) with the use of a divider.

Point B: The FD of fixed resolution, produces an output voltage. If the sweep time is 1ms for 500 MHz change in frequency and there are x bits, then the measurement speed of at least $e^{\frac{-3}{2^x}}$ seconds is required [13].

Point C: A low pass filter is needed to reject the high frequencies generated by abrupt transition of the FD output. This filter is of great importance in determining the loop bandwidth and characteristics. The loop bandwidth has to be narrow enough to allow fast locking and wide enough to permit fast acquisition.

The cut off frequency to be determined is a function of all the elements in the loop. It is not possible to determine this frequency before all these elements are known. The digitizing in the feedback loop makes it very difficult to analytically determine the frequency. A simulation of the system will give an indication of the values of the filter and the needed amplification at point D.

The noise of the VCO will not be improved if the low pass filter cut off frequency is too high.

Point D: This point is the error signal. The input signal is a ramp and therefore the error signal will reach a steady state error on one sweep. To obtain the wanted steady state value, an amplifier or preferably an integrator with gain is needed.

The digital FD is an expensive and relatively large component. A few techniques exist to replace the digital FD using relatively simple logic.

a) Monostable discriminator

Use the input signal present at A to trigger a monostable as shown in Figure 4.5. If the frequency increases, the number of pulses will also increase. The average voltage will therefore increase

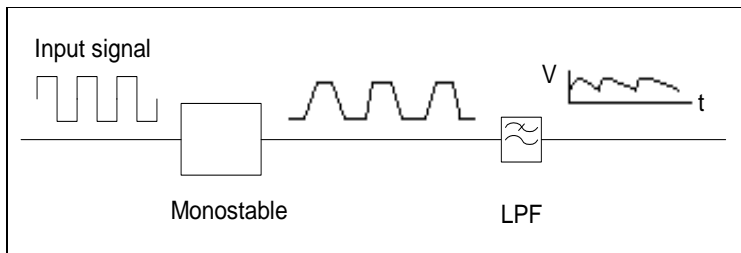


Figure 4.5 Monostable discriminator [13].

b) And-gate discriminator

Split the input signal in two, send the one channel through a delay line and compare the two channels with an and-gate as shown in Figure 4.6. The larger the delay, the shorter the pulses at the output of the and-gate. The average voltage will therefore decrease.

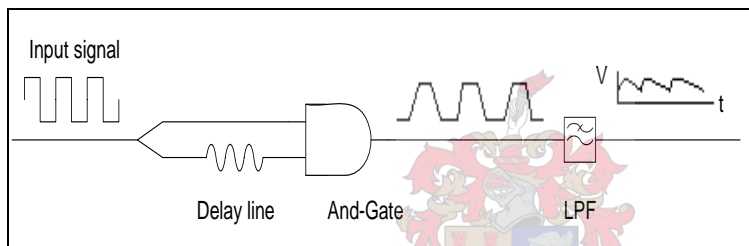


Figure 4.6 And-Gate Discriminator [13].

The average voltage of the output pulses is needed in both cases. This can be done with an integrator and sample and hold circuit. The number of pulses to integrate are not large enough to obtain sufficient differences between the highest and lowest frequencies.

A low - pass filter can also be used to obtain the average voltage. The linearity is directly dependant on the ripple at the output of the filter. A very high order low pass filter is necessary to get rid of the ripple at the output of the filter.

The pulses have relatively long rise and fall times and this will have a significant influence on the average value.

4.3.2 Analogue frequency discriminator technique

This method is similar to that of the digital method of the previous section where the digital FD is replaced by an analogue FD. There exists various methods of analogue discriminators of which the delay line is probably the best known (Figure 4.7).

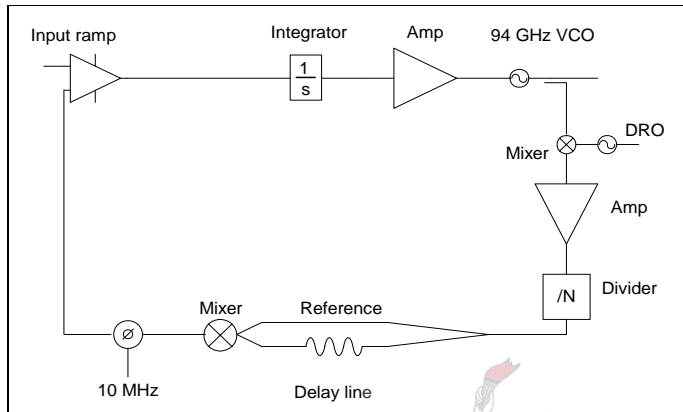


Figure 4.7 Phase-Locked Loop using a delay-line [13].

The one channel is used as a reference while the other is delayed by a specific time. The two signals are mixed and a constant frequency is obtained for a linear VCO output response. The phase of the output frequency is compared to that of a stable low frequency oscillator and the output is added to the input ramp. A crystal oscillator of 10 MHz can be used if the delay line can produce an output of 10 MHz.

The delay lines are normally realised by SAW's or optic fibre. The frequency range of the SAW is from 20 MHz to 1 GHz and a bandwidth of 50% can be achieved [13]. The insertion loss of this discriminator is high (40dB). This method is used by Phillips and a linearity of better than 0.1% is obtained [13].

Optic fibre is also used as a delay line. When the sweep frequency and time are specified, the delay time can be calculated to give a constant output frequency of 10 MHz after the phase detector. Optical cables have a delay time of typically 5 ns per metre. For a sweep time of typically 1 ms and a sweep frequency of 500 MHz, a delay of 20 μ s is needed. Such a cable will be about 4 km long. The fibre is typically 100 to 140 μ m thick and can be wound onto a cylinder with a radius of not smaller than 12cm.

The key specifications for analogue FD are the linearity, slope over a given frequency range, peak voltage and absolute output voltage for specific input frequencies. The output voltage of the phase comparator as a function of the phase difference is shown in Figure 4.8 Output voltage of the phase comparator [13].

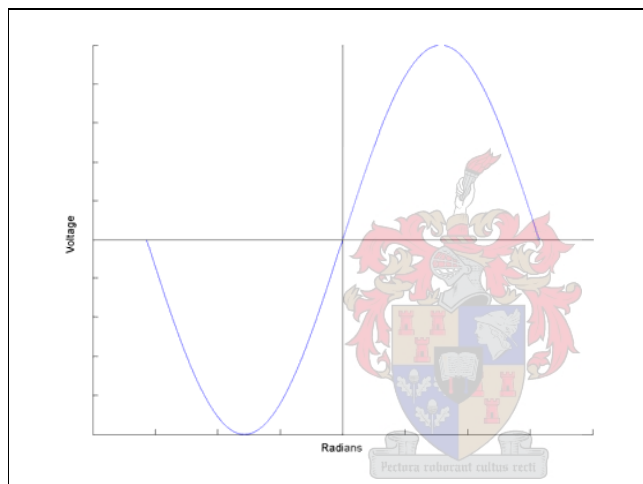


Figure 4.8 Output voltage of the phase comparator [13].

It is possible to use a non-linear amplifier in the configuration of the figure above to compensate for the non-linearity of the sinusoidal response. A linearity of 0.5% was obtained by this method [13]. The linearity should improve further if more than one of these amplifiers are added and/or multiplied.

4.4 Phase Lock Loop with Direct Digital Synthesizer

Figure 4.9 illustrates the principle of operation of this method in which the VCO is locked to the frequency of the DDS. If the output of the DDS is a ramp, the VCO will follow this response. The linearity of the DDS output will determine the linearity of the system.

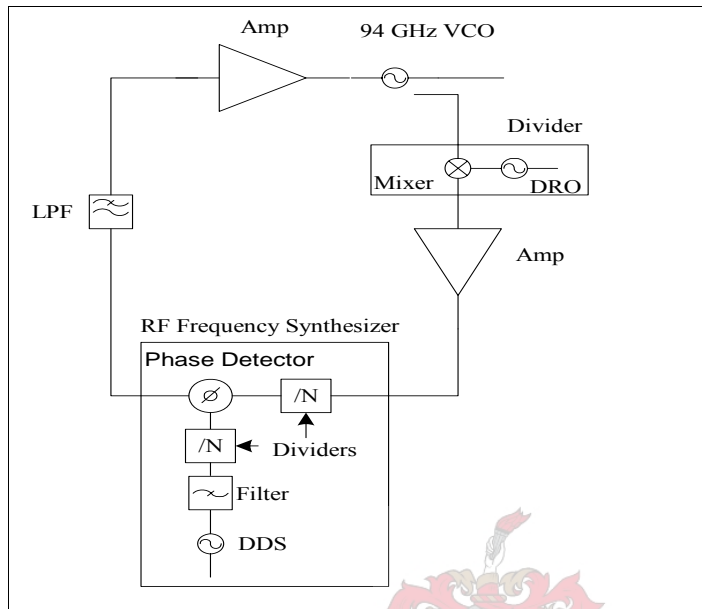


Figure 4.9 Phase Lock Loop with Direct Digital Synthesizer.

Philips achieved 0.03% linearity using the phase-locking technique [13].

4.5 Conclusion

To summarize the techniques discussed in this chapter:

1. Open loop linearization is dependant on the environmental stability of the VCO.
2. The desired linearity can be achieved with a digital FD. The available FD will determine the mixed down frequency and the dividing number (N). Digital discriminators are relatively large and expensive. Simple logic requires complex filtering and will not produce the required linearity.

3. Optic fibre may be used as a delay in a frequency locked loop. Analogue FD's are not linear enough to be used directly.
4. Phase-locking the VCO to a DDS is a solution which would produce the best linearity.

For this specific application the system is required to obtain a very good linearity. The PLL using a DDS will produce a very good linearity. This technique is chosen as the best for this application.



5 Phase Lock Loop using a Direct Digital Synthesizer

This chapter describes the Phase Lock Loop (PLL) technique using a Direct Digital Synthesizer (DDS). The basic principles of a PLL are discussed with a detailed look at the individual components characterizing and determining PLL model parameters. The importance and design considerations of the Low Pass Filter (LPF) in the PLL are discussed.

5.1 Basic Principles of a PLL

The basic idea of a PLL is that if one injects a sinusoidal into the reference input, the internal oscillator in the loop will lock to the reference sinusoid in such a way that the frequency and phase differences between the reference sinusoid and the internal sinusoid will be driven to some constant value or 0 [15]. The internal sinusoid then represents a filtered or smoothed version of the reference sinusoid. Figure 5.1 illustrates a general PLL block diagram.

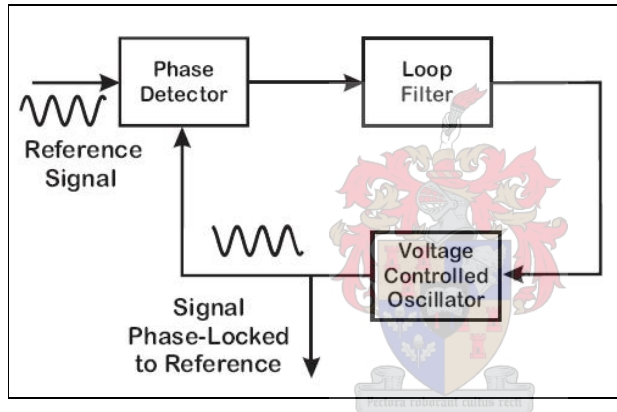


Figure 5.1 A General PLL block diagram [15].

5.1.1 PLL Operation

The PLL can be analysed as a feedback control system as shown in Figure 5.2. With no signal applied to the system, the VCO control voltage, $V_d(t)$, is equal to zero. The VCO operates at a set frequency, f_0 , which is known as the free running

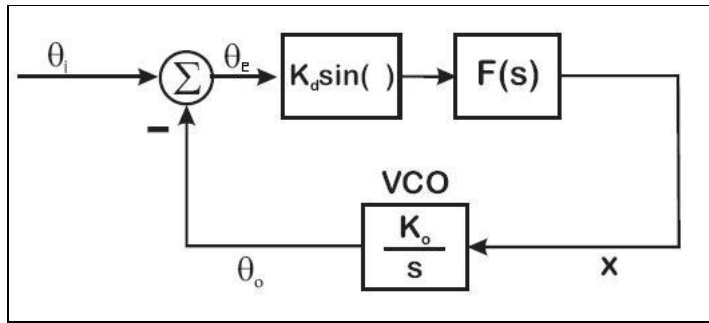


Figure 5.2 PLL illustrated as a feedback control system [15].

frequency. When an input signal is applied to the system, the phase comparator compares the phase and frequency of the input with the VCO frequency and generates an error voltage, $V_e(t)$, that is related to the phase and the frequency difference between the two signals. This error voltage is then filtered, amplified, and applied to the control terminal of the VCO.

In this manner the voltage $V_d(t)$ forces the VCO frequency to vary in a direction that reduces the frequency difference between ω_0 and the input signal. If the input frequency ω_i is sufficiently close to ω_0 , the feedback nature of the PLL causes the VCO to synchronise or lock with the incoming signal. Once in lock, the VCO frequency is identical to the input signal except for a finite phase difference [15].

This net phase difference of θ_e where

$$\theta_e = \theta_0 - \theta_i \quad (5-1)$$

is necessary to generate the corrective error voltage V_d to shift the VCO frequency from its free-running value to the input signal frequency ω_i and thus keep the PLL in lock. This self-correcting ability of the system also allows the PLL to track the frequency changes of the input signal once it is locked. The range of frequencies over which the PLL can maintain lock with an input signal is defined as the “lock range” of the system. The band of frequencies over which the PLL can acquire lock with an incoming signal is known as the

“capture range” of the system and is never greater than the lock range. Another means of describing the operation of the PLL is to observe that the phase comparator is in actuality a multiplier circuit that mixes the input signal with the VCO signal. This mix produces the sum and the difference frequencies $\omega_1 \pm \omega_0$ shown in Figure 5.3.

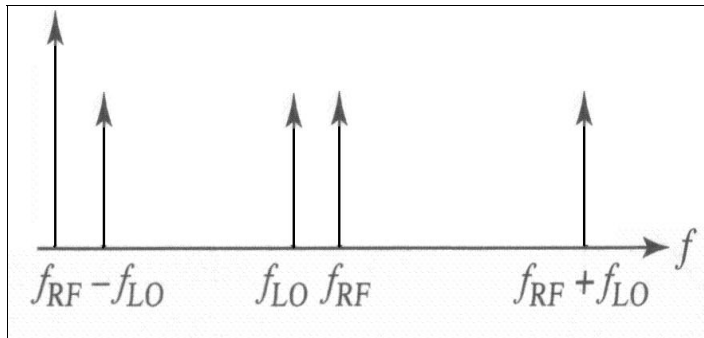


Figure 5.3 Frequency conversion using a mixer [16].

When the loop is in lock, the VCO duplicates the input frequency so that the difference frequency component ($\omega_0 \bullet \omega_1$) is zero; hence, the output of the phase comparator contains only a DC component. The low-pass filter removes the sum frequency component ($\omega_0 + \omega_1$) but passes the DC component, which is then amplified and fed back to the VCO.

5.1.2 Lock and Capture

Consider now the case where the loop is not yet in lock. The phase comparator mixes the input and VCO signals to produce sum and difference components. However, the difference component may fall outside the band edge of the low-pass filter and be removed along with the sum frequency component. If this is the case, no information is transmitted around the loop and the VCO remains at its initial free-running frequency. As the input frequency approaches that of the VCO, the frequency of the difference component decreases and approaches the band edge of the LPF. Now some of the difference component is passed, which tends to drive the VCO towards the frequency of the input signal. This, in turn, decreases the frequency of the difference component and allows more information to be transmitted through the LPF to the VCO. Figure 5.4 Shows the lockup time as the VCO frequency approaches the reference frequency.



Figure 5.4 Lockup time characteristic at higher cut off frequency [17].

This is essentially a positive feedback mechanism which causes the VCO to snap into lock with the input signal. Capture range can assume any value within the lock range and depends primarily upon the band edge of the LPF together with the closed loop gain of the system.

When the loop is in lock, the difference frequency component at the output of the phase comparator (error voltage) is DC and will always be passed by the LPF. Thus the lock range is limited by the range of the error voltage that can be generated and the corresponding VCO frequency deviation produced. The lock range is essentially a DC parameter and is not affected by the band edge of the LPF.

5.1.3 The capture transient

The capture process is highly complex and does not lend itself to simple mathematical analysis. However, a qualitative description of the capture mechanism may be given as follows. Since the frequency is the time derivative of phase, the frequency and the phase errors in the loop can be related as [15]

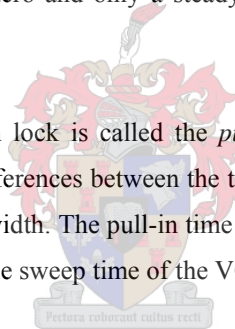
$$\Delta\omega = \frac{d\theta_e}{dt} \quad (5-2)$$

where $\Delta\omega$ is the instantaneous frequency separation between the signal and VCO frequencies and θ_e is the phase difference between the input and VCO signals.

If the feedback loop of the PLL were opened between the LPF and the VCO control input, then for a given condition of ω_0 and ω_1 the phase comparator output would be a sinusoidal beat note at a fixed frequency $\Delta\omega$. If ω_0 and ω_1 were sufficiently close in frequency, this beat note would appear at the filter output with negligible attenuation.

Now suppose that the feedback loop is closed by connecting the LPF output to the VCO control input. The VCO frequency will be modulated by the beat note. When this happens, $\Delta\omega$ itself will become a function of time. If, during this modulation process, the VCO frequency moves closer to ω_1 then $\frac{d\theta_e}{dt}$ decreases and the output of the phase comparator becomes a slowly varying function of time. Similarly, if the VCO is modulated away from ω_1 , $\frac{d\theta_e}{dt}$ increases and the error voltage becomes a rapidly varying function of time. Under these conditions the beat note waveform no longer looks sinusoidal; it looks like a series of aperiodic cusps. Because of its asymmetry, the beat note waveform contains a finite DC component that pushes the average value of the VCO towards ω_1 , and lock is established. When the system is in lock, $\Delta\omega$ is equal to zero and only a steady-state DC error voltage remains.

The total time taken by the PLL to establish lock is called the *pull-in time*. Pull-in time depends on the initial frequency and phase differences between the two signals as well as on the overall loop gain and low-pass filter bandwidth. The pull-in time is very important in this application, because this time will determine the sweep time of the VCO.



5.1.4 Effect of the Loop Filter

In the operation of the loop, the loop filter serves a dual function. First, by attenuating the high frequency error components at the output of the phase comparator; second, it provides a short term memory for the PLL and ensures a rapid capture of the signal if the system is thrown out of lock due to a noise transient [15].

5.2 Component characteristics in a PLL

The most basic block diagram of a PLL is shown in Figure 5.1. This diagram shows the components that every PLL must have, namely [15]:

1. A phase detector (PD). This is a nonlinear device whose output contains the phase difference between the two oscillating input signals.
2. A voltage controlled oscillator (VCO). This is another nonlinear device which produces an oscillation whose frequency is controlled by a lower frequency input voltage.
3. A loop filter (LF). While this can be omitted, resulting in what is known as a first order PLL, it is always conceptually there since PLL's depend on some sort of low pass filtering in order to function properly.
4. A feedback interconnection. Namely the phase detector takes as its input the reference signal and the output of the VCO. The output of the phase detector, the phase error, is used as the control voltage for the VCO. The phase error may or may not be filtered.

The following sections will give a brief description of each of the components in the PLL.

5.2.1 Phase Detectors

A phase detector is a dc-coupled mixer which provides an output voltage that is dependant on the phase difference between two input signals. A simple analogue phase detector is shown in Figure 5.5.

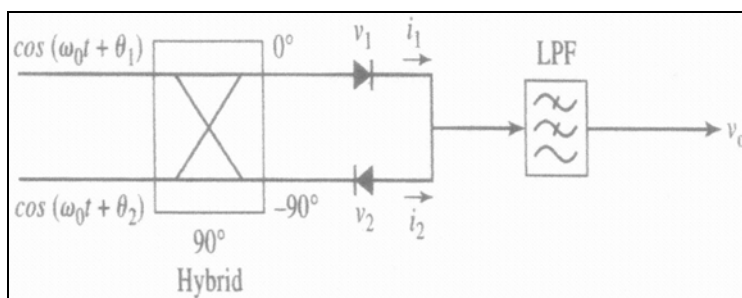


Figure 5.5 Circuit diagram for an analogue phase detector [16].

After the loop is locked, f_o will be exactly equal to f_i ($f_o = f_i$) by definition of “locked,” and only a phase difference can exist between the two phase-detector input signals. A phase difference between the two input signals results in a dc voltage V_d , which is proportional to the phase difference, $\theta_e = \theta_i - \theta_o$ [15]. This is first shown mathematically, then graphically.

A mixer performs the mathematical function of multiplication. Thus for sinusoidal inputs

$$\begin{aligned} v_d &= A \sin(\omega_i t + \theta_i) \times 2 \cos(\omega_o t + \theta_o) \\ &= A \sin[(\omega_i t + \theta_i) - (\omega_o t + \theta_o)] + A \sin[(\omega_i t + \theta_i) + (\omega_o t + \theta_o)] \end{aligned} \quad (5-3)$$

When phase-locked, $\omega_o = \omega_i$, the second harmonic term, $A \sin[2\omega_o t + \theta_o + \theta_i]$, is filtered out, leaving

$$V_d = A \sin(\theta_i - \theta_o) \quad (5-4)$$

This voltage is directly proportional to the input signal amplitude and, more importantly, the phase error θ_e if the signal amplitude is held constant. Indeed, for small θ_e , this transfer function is linear. The comments of the last two sentences assume that the VCO voltage is much larger in amplitude than the input signal. If the VCO amplitude is not strong enough to be considered a switching function, or the signal level is so strong as to be comparable in level to the VCO voltage, then A of Equation (5.4) will be proportional to one-half the product of the VCO and input signal levels.

5.2.1.1 Phase Detector Gain

The phase detector just discussed is a mixer, which mathematically is a multiplier, with a direct-coupled output. When the loop PLL is locked and has no stress on it, the voltage applied to the VCO must be zero, so the phase detector output must also be zero. Thus the phase detector (locked-loop) operates with a 90° offset, but this is really no different than a circuit-bias offset. The locked loop phase detector input-output (transfer) characteristic is similar to the FM discriminator S-curve. However, the PD characteristic is a continuous sinusoid repeating every 2π radians. Also, during the tracking mode, operation is limited to the portion of the curve between $\pm \frac{\pi}{2}$ where $|\theta_e| < \frac{\pi}{2}$. This is because, for θ_e between

$\frac{\pi}{2}$ and $\frac{3\pi}{2}$, the slope of the PD characteristic is negative, resulting in an unstable (regenerative feedback) loop [15]. For sinusoidal inputs it is clear from figure that the slope of the phase detector characteristic curve,

$$V_d = A \sin \theta_e \quad (5-5)$$

is not constant. In fact, it rises with a maximum slope at $\theta_e = 0$, and levels off to a slope of zero (no gain) at $\theta_e = \frac{\pi}{2}$ rad. Since we are usually interested in loop behaviour for small θ_e , let's find the slope (gain) at $\theta_e = 0$. A proof of this is given,¹ but it turns out that the peak voltage A is the volts-per-radian gain of this phase detector because the tangents to the peak and the PD curve at $\theta_e = 0$ intersect at 1 rad, as seen in Figure 5.6. Therefore, the gain of the analog phase detector is

$$k_\phi = \frac{2A}{\pi} \quad (5-6)$$

5.2.1.2 Digital Phase Detectors

This section will explore phase detectors constructed from digital logic for which the initial reduction to baseband relies on arguments of pulse-width modulation and averaging [15]. While these phase detectors have worse noise performance than the classic mixing detectors, they often have better pull in range and are much more manufacturable, especially for high speed applications. Furthermore, most of these phase detectors have the advantage that their low frequency response is actually linear over some range rather than sinusoidal.



Analysis of digital phase detectors requires a different view from that of classical mixing detectors. First of all, while the exact behaviour of these digital phase detectors is necessarily nonlinear, the low frequency behaviour is often linear. Secondly, the circuit of the phase detectors is constructed more to deal with specific circuit conditions than to make analysis simpler. Finally, no one type of phase detector is best for all situations. Thus, vastly different

¹ The slope of the PD curve, $V_d(\theta) = A \sin \theta_e$, at the origin is

$$\frac{d}{d\theta} [A \sin \theta_e] |_{\theta_e=0} = A \cos 0 = A$$

circuit designs are chosen to implement largely the same functionality for different applications.

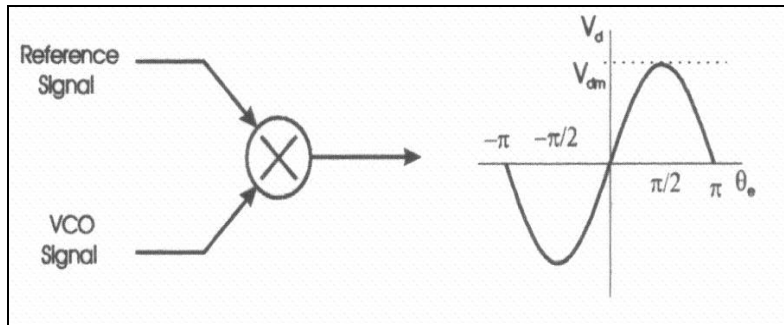


Figure 5.6 Classical mixing phase detector [15].

The mixing phase detector shown in Figure 5.6 and discussed in section 5.1, has superior noise performance to all the other detectors discussed here [15], due to the fact that it operates on the entire amplitude of the input and VCO signals, rather than quantifying them to 1 bit. Balanced mixers are best suited for PLL applications in the microwave frequency range as well as in low noise frequency synthesizers. However, this results in a loop whose gain is dependant upon the signal amplitude. Furthermore, nonidealities in the circuit implementation of the mixer results in responses that are far from linear. When noise is not an issue, it is advantageous to move to a detector that has immunity to these effects.

5.2.1.3 XOR

For a variety of reasons, it may be desirable to have a loop which does not produce a sinusoidal clock but instead a square wave clock. If one over-drives the mixer circuit, that is if one uses signals so large that the amplifiers saturate, the output signals stop looking like sinusoidal and start looking like Walsh functions (rectangular signals). Such a phase detector is shown in Figure 5.7.

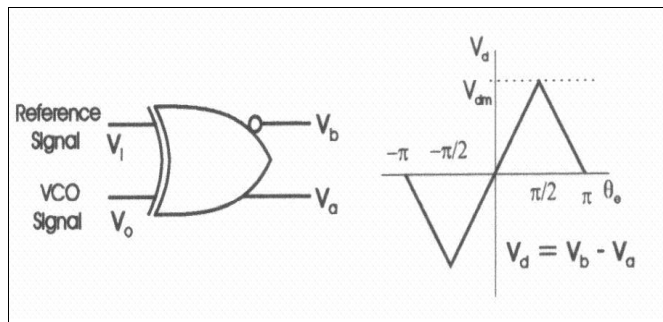


Figure 5.7 Phase detector using an XOR gate [15].

Understanding the output of such a phase detector relies on a combination of averaging analysis and heuristics. However, one of the more interesting features of such a phase detector is that it can be implemented using an Exclusive-OR (XOR) gate as shown in Figure 5.7. One advantage of such a phase detector is that the loop gain is now independent of input signal amplitude. Furthermore, an XOR phase detector's response can have a larger linear range than a sinusoidal detector (mixer). The disadvantage is that the linearity of the baseband response is affected by the relative duty cycle of the input and VCO signals [15].

5.2.1.4 Two state Phase Detectors

To eliminate the duty cycle dependence of the XOR phase detector, detectors using logic gates can be used. An example of this, found in Wolaver [15], is shown in Figure 5.8. The addition of the two flip flops to the XOR gate has several results. First, the phase detector is only sensitive to the rising edges of the input signals, rather than their duty cycles. Secondly, the linear region of the phase detector is expanded to $\pm\pi$ from $\pm\frac{\pi}{2}$. Finally, the phase detector is no longer memoryless. Thus, noise spikes that are large enough to trigger change of state have a larger effect than they do with

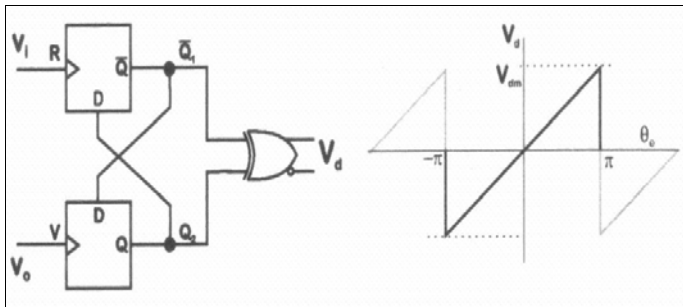


Figure 5.8 Two state phase detector using logical gates [15].

the XOR phase detector. The resulting baseband component of the phase detector output now has a sawtooth, rather than a triangle wave response, and so this detector is often called a sawtooth detector.

5.2.1.5 Phase-Frequency Detectors

An extremely popular phase detector is the combination of the tri-state phase-frequency detector (PFD) with a charge pump shown in Figure 5.9.

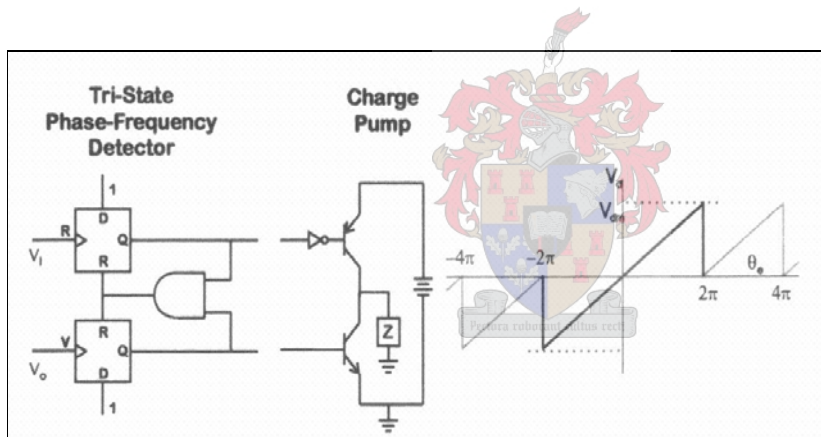


Figure 5.9 Tri-state phase-frequency detector [15].

The charge pump can be viewed as a 3 position switch controlled by the phase-frequency detector. The action of the charge pump is to alleviate any loading of the phase detector in

driving the rest of the circuit. This allows the response to be smoother than without the charge pump.

5.2.2 Voltage-Controlled Oscillator (VCO)

The actual clock generated by a PLL comes from the VCO. The VCO is a nonlinear device which generates a periodic oscillation. The frequency of this oscillation can be controlled by modulating some control voltage. In a PLL, the control voltage corresponds to some filtered form of the phase error. In response to this, the VCO adjusts its frequency. As the VCO frequency is slewed by the control voltage, the phase error is driven towards 0. This frequency adjustment to achieve phase lock results in the model of a VCO as an integrator.

5.2.3 Loop Filters

As the vast majority of PLL's are second order and as the action of the VCO are modelled as an integrator, loop filters are typically first order. All PLL's depend on some sort of low pass filter in order to function properly. Loop filters will be discussed in more detail in section 5.4.

5.2.4 Amplifier

The function of the dc amp is to increase the loop gain by amplifying the phase detector output voltage. The bandwidth of the dc amp must be very high compared to the loop bandwidth, or loop instability will result – even to the point of oscillation due to excessive phase shift around the loop, which would produce positive (regenerative) feedback.

5.3 Determining PLL model parameters

Since the PLL is basically an electronic servo loop, many of the analytical techniques developed for control systems are applicable to phase-locked systems. Whenever phase lock is established between $v_i(t)$ and $v_o(t)$ the linear model of Figure 5.2 can be used to predict the performance of the PLL system. Here θ_i and θ_o represent the phase angles associated with the input/output wave shapes, respectively; $F(s)$ represents a generalised voltage transfer function for the low-pass filter in the s complex frequency domain; and K_d and K_o are

conversion gains of the phase comparator and VCO respectively, each having units as shown.

The $\frac{1}{s}$ term associated with the VCO accounts for the inherent 90° phase shift in the loop since the VCO converts a voltage to a frequency and since phase is the integral of frequency.

5.3.1 Mathematically defining PLL operation

As mentioned previously, the phase comparator is basically an analogue multiplier that forms the product of an RF input signal, $V_i(t)$, and the output signal, $V_o(t)$, from the VCO. Assume that the two signals to be multiplied can be described by

$$V_i(t) = V_1 \sin(\omega_1 t) \quad (5-7)$$

$$V_o(t) = V_0 \sin(\omega_0 t + \theta_e) \quad (5-8)$$

where ω_0 , ω_1 and θ_e are the frequency and phase difference (or phase error) characteristics of interest. The product of these two signals is an output voltage given by

$$V_e(t) = K_1 V_1 V_0 \sin(\omega_1 t) \sin[\omega_0 t + \theta_e] \quad (5-9)$$

where K_1 is an appropriate dimensional constant

The two cases of an unlocked loop ($\omega_1 \neq \omega_0$) and of a locked loop ($\omega_1 = \omega_0$) are now considered separately [15].

5.3.2 Unlocked state ($\omega_1 \neq \omega_0$)

When the two frequencies to the phase comparator are not synchronised, the loop is not locked. Furthermore, the phase angle difference θ_e in equation 5.8 and 5.9 is meaningless for this case since it can be eliminated by appropriately choosing the time origin (give example).

Using trigonometric identities, equation 5.9 can be written as

$$V_e(t) = \frac{K_1 V_1 V_0}{2} [\cos(\omega_1 - \omega_0)t - \cos(\omega_1 + \omega_0)t] \quad (5-10)$$

When $V_e(t)$ is passed through the LPF, $F(s)$, the sum frequency component is removed, leaving

$$V_e(t) = K_2 V_1 V_0 [\cos(\omega_1 - \omega_0)t] \quad (5-11)$$

After amplification, the control voltage for the VCO appears as

$$V_d(t) = AK_2 V_1 V_0 [\cos(\omega_1 - \omega_0)t] \quad (5-12)$$

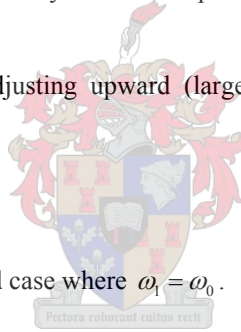
This equation shows that a beat frequency effect is established between ω_1 and ω_0 , causing the VCO's frequency to deviate by $\pm\Delta\omega$ from ω_0 in proportion to the signal amplitude ($AK_2 V_1 V_0$) passing through the filter. If the amplitude of V_1 is sufficiently large and if signal limiting or saturation does not occur, the VCO output frequency will be shifted from ω'_0 by some $\Delta\omega$ until lock is established where

$$\omega_1 = \omega_0 = \omega'_0 \pm \Delta\omega \quad (5-13)$$

If lock cannot be established, then either V_1 is too small to drive the VCO to produce the necessary $\pm\Delta\omega$ deviation or ω_1 is beyond the dynamic range of the VCO [15].

Remedies for these no lock conditions are:

- a) Increase V_1 either internally or externally to the loop by providing additional amplification
- b) Increase the internal loop gain by adjusting upward (larger -3dB frequency) the response of the LPF.
- c) Shift ω'_0 closer to the expected ω_1 .



Establishing frequency lock leads to the second case where $\omega_1 = \omega_0$.

5.3.3 Locked state ($\omega_1 = \omega_0$)

When ω_1 and ω_0 are frequency synchronised, the output signal from the phase comparator for $\omega_1 = \omega_0$ and a phase shift of θ_e is

$$V_e(t) = \frac{K_1 V_1 V_0}{2} [\cos \theta_e - \cos(2\omega t + \theta_e)] \quad (5-14)$$

The LPF removes the high frequency, AC component of $V_e(t)$, leaving only the DC

component. Thus,

$$v_f(t) = K_2 V_1 V_0 \cos \theta_e \quad (5-15)$$

After amplification the DC voltage driving the VCO and maintaining lock within the loop is

$$v_d(t) = V_D = AK_2 V_1 V_0 \cos \theta_e \quad (5-16)$$

Suppose ω_1 and ω_0 are perfectly synchronised to the free running frequency ω'_0 . In this case, V_D will be zero, indicating that θ_e must be $\pm 90^\circ$. Thus V_D is proportional to the phase difference or phase error between θ_i and θ_o centered about a reference phase angle of $\pm 90^\circ$. If ω_1 changes slightly from ω'_0 , the first effect will be a change in θ_e from $\pm 90^\circ$. V_D will adjust and settle out to some nonzero value to correct ω_0 ; under this condition frequency lock is maintained with $\omega_1 = \omega_0$. The phase error will be shifted by some amount $\Delta\theta$ from the reference phase angle of $\pm 90^\circ$. This concept can be simplified by redefining θ_e as

$$\theta_e = \theta_r \pm \Delta\theta \quad (5-17)$$

where θ_r is the inherent, reference phase shift of $\pm 90^\circ$ and $\Delta\theta$ the departure from this reference value. Now the VCO control voltage becomes

$$\begin{aligned} V_D &= AK_2 V_1 V_0 \cos(\theta_r \pm \Delta\theta) \\ &= \pm AK_2 V_1 V_0 \sin(\Delta\theta) \end{aligned} \quad (5-18)$$

Since a sinusoidal function is odd, a momentary change in $\Delta\theta$ contains information about which way to adjust the VCO frequency to correct and maintain the locked condition. The maximum range over which $\Delta\theta$ changes can be tracked as -90° to 90° . This corresponds to a θ_e range from 0° to 180° . In addition to being an error signal, V_D , represents the demodulated output FM input applied as $V_{in}(t)$ assuming a linear VCO characteristic. Thus, FM demodulation can be accomplished with the PLL without inductively-tuned circuits that are employed with conventional detectors [15].

5.3.4 Modeling the PLL system with various low-pass filters

The open-loop transfer function for the PLL is

$$T(s) = \frac{K_v F(s)}{s} \quad (5-19)$$

Using linear feedback analysis techniques, and assuming that the VCO is in the forward path, the closed-loop transfer characteristics $H(s)$ can be related to the open-loop performance as

$$H(s) = \frac{T(s)}{1+T(s)} \quad (5-20)$$

and the roots of the characteristic system polynomial can be readily determined by root locus techniques [15].

From equation 5.19 and 5.20, it is apparent that the transient performance and frequency response of the loop is heavily dependant upon the choice of filter and its corresponding transfer characteristic, $F(s)$.

5.4 Low Pass Filter Design

5.4.1 Zero order filter

The simplest case is that of the first-order loop where $F(s)=1$ (no filter). The closed-loop transfer function of equation 5.20 then becomes

$$H(s) = \frac{K_v}{s + K_v} \quad (5-21)$$

Deleted: $T(s) = \frac{K_v}{s + K_v}$

This transfer function gives the root locus as a function of the total loop gain K_v and the corresponding frequency response as shown in Figure 5.10.

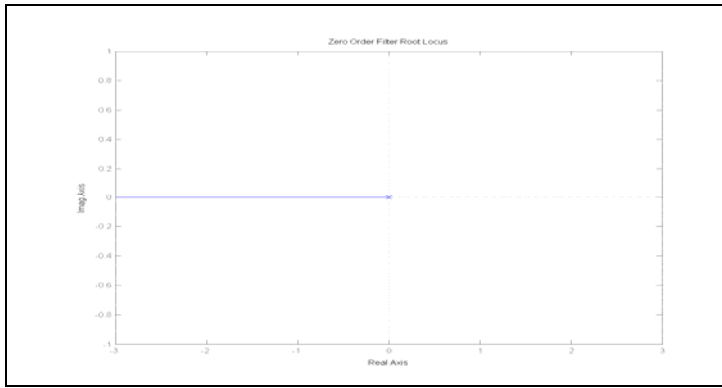


Figure 5.10 Simulated zero-order root locus [19].

The open-loop pole at the origin is due to the integrating action of the VCO. Note that the frequency response is actually the amplitude of the difference frequency component versus modulating frequency when the PLL is used to track a frequency modulated input signal. Since there is no LPF in this case, sum frequency components are also present at the phase comparator output and must be filtered outside of the loop if the difference frequency component (demodulating FM) is to be measured.

5.4.2 First-order filter

With the addition of a single-pole low-pass filter shown in Figure 5.11, $F(s)$ of the form

$$F(s) = \frac{1}{1 + \tau_1 s} \quad (5-22)$$

where $\tau_1 = R_1 C_1$, the PLL becomes a second-order system with root locus shown in Figure 5.12.

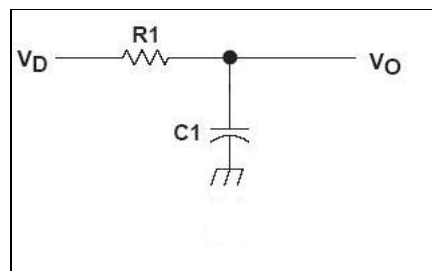


Figure 5.11 First-order low-pass filter.

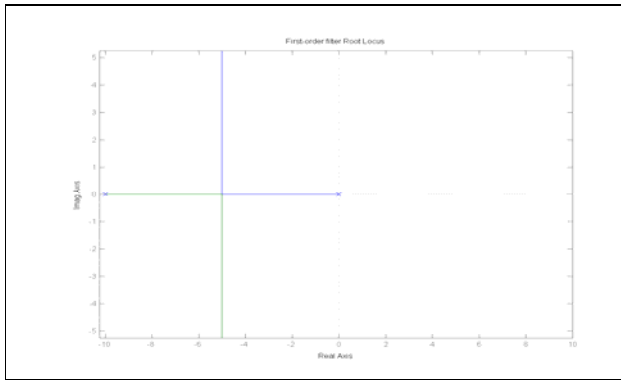


Figure 5.12 Simulated first-order filter root locus [19].

Again, an open-loop pole is located at the origin because of the integrating action of the VCO. Another open-loop pole is positioned on the real axis at $-\frac{1}{\tau_1}$ where τ_1 is the time constant of the low-pass filter.

One can make the following observations from the root locus characteristics of Figure 5.12 [15].

1. As the loop gain K_v increases for a given choice of τ_1 , the imaginary part of the closed-loop poles increases; thus, the natural frequency of the loop increases and the loop becomes more and more underdamped.
2. If the filter time constant is increased, the real part of the closed-loop pole becomes smaller and the loop damping is reduced.

As in any practical feedback system, excess shifts or non-dominant poles associated with the blocks within the PLL can cause the root loci to bend toward the right half plane. This is likely to happen if either the loop gain or filter time constant is too large and may cause the loop to break into sustained oscillation.

5.4.3 First order lag-lead filter

The stability problem can be eliminated by using a lag-lead type of filter, as indicated in Figure 5.13.

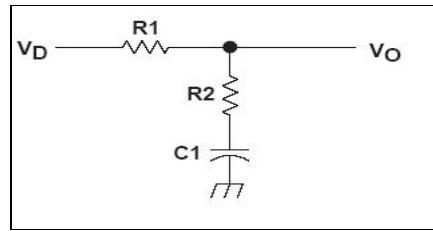


Figure 5.13 Lag-Lead low-pass filter.

This type of filter has the transfer function

$$F(s) = \frac{1 + \tau_2 s}{1 + (\tau_1 + \tau_2)s} \quad (5-23)$$

where $\tau_1 = R_1 C$ and $\tau_2 = R_2 C$. By proper choice of R_2 , this type of filter confines the root locus shown in Figure 5.14 to the left half-plane and ensures stability.

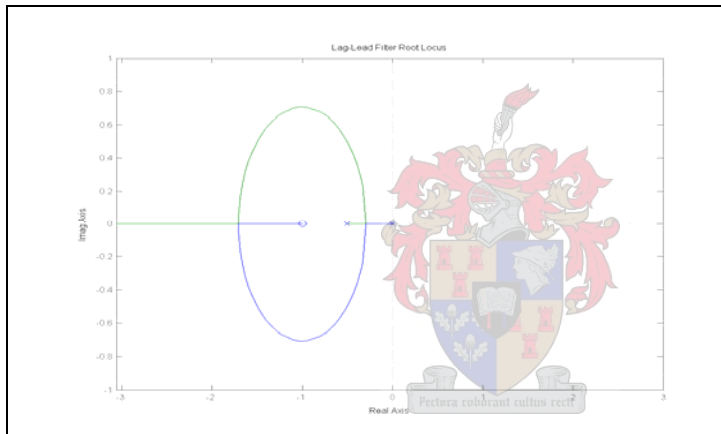


Figure 5.14 Simulated lag-lead filter root locus [19].

The lag-lead filter gives a frequency response dependant on the damping, which can now be controlled by the proper adjustment of τ_1 and τ_2 . In practice, this type of filter is important because it allows the loop to be used with a response between that of the first- and second-order loops and it provides an additional control over the loop transient response. If $R_2 = 0$, the loop behaves as a second-order loop and as $R_2 \rightarrow \infty$, the loop behaves as a first-order

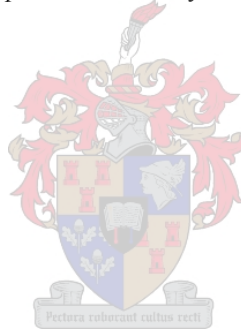
loop due to a pole-zero cancellation. However, as first-order operation is approached, the noise bandwidth increases since the high frequency error components in the loop are now attenuated to a lesser degree [15].

5.4.4 Second- and Higher-Order Filters

Second- and higher-order filters, as well as active filters, occasionally are designed and incorporated within the PLL to achieve a particular response not possible or easily obtained with zero- or first-order filters. Adding more poles and more gain to the closed-loop transfer function reduces the inherent stability of the loop. Thus the designer must exercise extreme caution and utilize complex stability analysis if second-order (and higher) filters or active filters are to be considered.

5.5 Conclusion

A basic PLL consists of a phase detector, a loop filter, a stable reference signal, a VCO and some form of amplification. The phase-frequency detector, a lag-lead low-pass filter, a DDS and the 94.5 GHz VCO will be used for the system implementation. The next chapter introduces the implementation of the PLL to improve the linearity of the 94.5 GHz VCO.



6 System Implementation

In this chapter the implementation of the PLL technique to improve the existing systems linearity is described. The linearization scheme is shown in Figure 6.1. An important design consideration is to note that the 94.5 GHz VCO needs to be mixed down to a frequency range suitable for the PLL components. This is done by using a harmonic mixer to produce an IF of 2 and 3 GHz. The IF will then be locked to the reference frequency of a DDS.

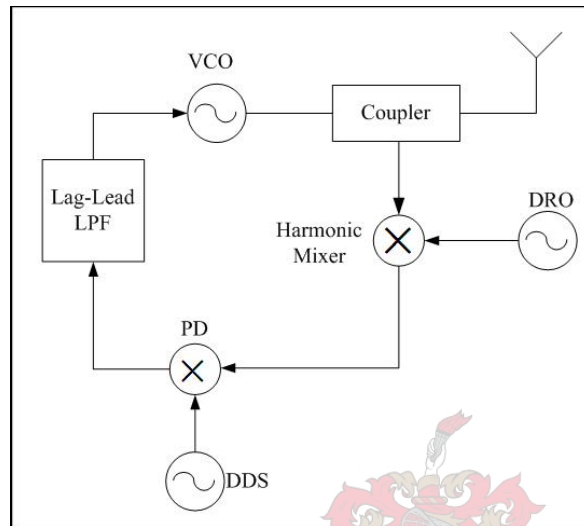


Figure 6.1 Block diagram of linearization system.

Important components in the PLL are the VCO, phase-detector, harmonic mixer, DRO, DDS, and the low-pass filter. The first component that will be looked at is the phase detector.

6.1 Phase Detector

The PD is a nonlinear device whose output contains the phase difference between two oscillating input frequencies as discussed in section 5.2.1. The output of the PD is a changing voltage in accordance to the phase difference between the two signals. The PD that is implemented in the system, is a low-noise digital phase frequency detector (PFD). The PFD was chosen because of the advantages over other PD discussed in section 5.2. The PFD is part of the Analog Devices ADF4113 RF PLL synthesizer used for the implementation. This

chip includes an N-divider for the VCO input, an R-divider for the reference DDS input and a charge pump to amplify the output control voltage as shown in Figure 6.2.

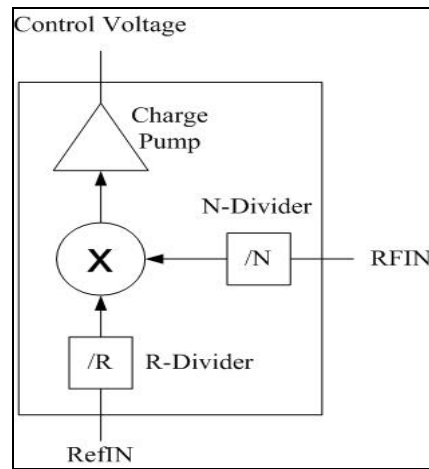


Figure 6.2 Block diagram of the ADF4113 implementation.

The following table gives some specifications of the RF PLL Frequency Synthesizer chip.

Table 6.1 Specifications of the ADF4113.

Parameter	Min. value	Max. value	Unit
Power Supply	2.7	5.5	V
RF Input Frequency	0.2	4	GHz
RF Input Sensitivity	-15	0	dBm
REFIN Input Frequency	5	104	MHz
REFIN Input Sensitivity	-5	-	dBm
PD Frequency	-	55	MHz

There are three on-chip registers (Reference Counter Latch, AB Counter Latch, and a Function Latch) which are controlled via a simple 3-wire interface. This control is done by using an AVR® ATmega8. The Reference Counter Latch is used to set the value of the REFIN divider. The AB Counter Latch is used to set the RF input divider. The following equation gives the total dividing number of the RF input frequency.

$$N = BP + A \quad (6-1)$$

where P is the prescaler value.

The Function Latch is used to set the prescaler value, the current setting, and the polarity of the output of the charge pump. The prescaler values are calculated by using the following equation

$$f_{VCO} = \frac{N \times f_{REFIN}}{R} \quad (6-2)$$

6.2 Harmonic Mixer

The harmonic mixer is used to mix the 94.5 GHz VCO output signal down to 2-3 GHz, depending on the varactor tuning voltage. This is done by using the CTI DRO discussed in section 2.6.4 as reference frequency shown in Figure 6.3.

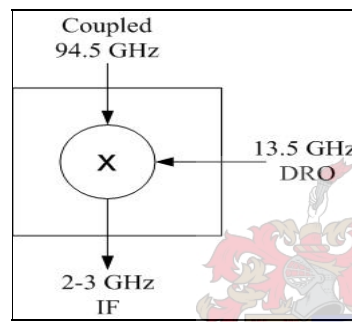


Figure 6.3 Block diagram of harmonic mixer.

The centre frequency of the DRO is measured as 13.142 GHz. To mix the 94.5 GHz reference down to 2.5 GHz the 7th harmonic of the DRO is used.

The output power of the mixer is measured as -40 dBm. From Table 6.1 it is clear that this signal level is at least 25 dB lower than the minimum allowable RF input signal of the ADF4113. It is therefore necessary to amplify this signal to an allowable level.

6.3 Amplifier Implementation

If the RF input signal to the ADF4113 has to be -5 dBm, the amplification needed after the mixer will be 30 dB. This large amplification means that any small signal at the input of the

amplifier, could cause the amplifier to be unstable, or oscillate. To avoid oscillation, good care has to be taken when defining the ground plane of the amplifier system. The shortest possible path from every component to ground has to be attained to avoid this kind of oscillation. For this amplifier two Mini-Circuits ERA-5 Monolithic Amplifiers are used in cascade to give 30 dB gain. The following figure represents the biasing of the amplifier.

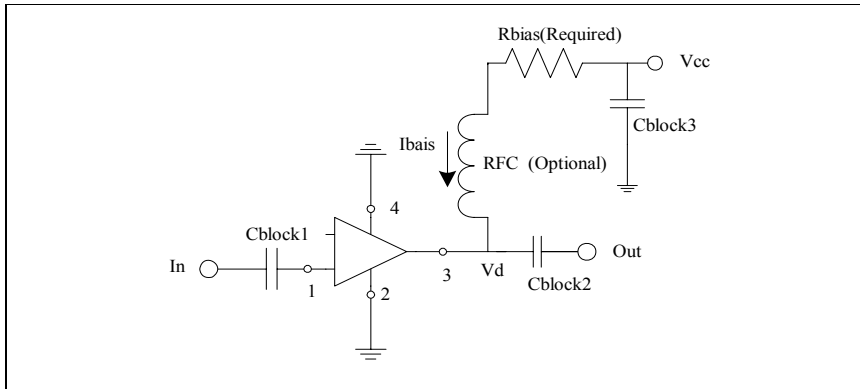


Figure 6.4 Typical biasing configuration [18].

In Figure 6.4 *Cblock1* and *Cblock2* are low frequency block capacitors. Their values are determined by the following equation

$$C = \frac{1}{2\pi fZ} \quad (6-3)$$

where Z is the impedance at the frequency, f . For $Z = 500\Omega$ and $f = 25\text{MHz}$, the value of *Cblock1* and *Cblock2* is ± 10 pF.

Figure 6.5 shows the IF amplifier implemented. The gain is measured to be 32 dB over a frequency band of 2-3 GHz with a maximum ripple of 0.5 dB across the band.

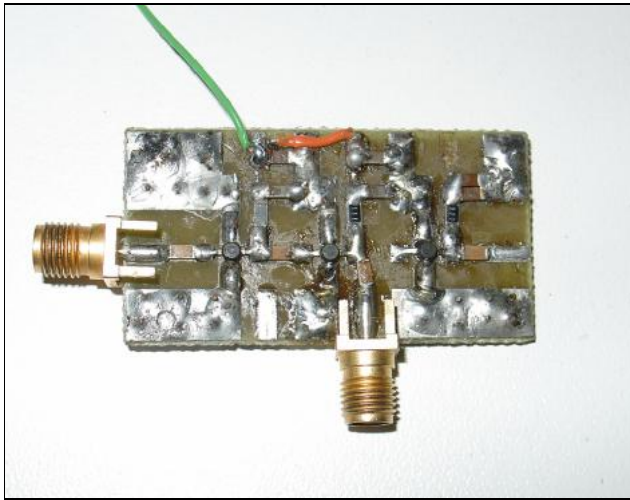


Figure 6.5 Photo taken of IF amplifier.

6.4 DDS Implementation

A CMOS 180 MHz DDS Synthesizer chip AD9851 from Analog Devices is used as the reference frequency for the ADF4113. When referenced to an accurate clock source, the AD9851 generates a stable frequency and phase-programmable digitized analog output sine wave. The AD9851 is programmed with the Atmega8 by loading of the frequency tuning, control and phase words asynchronously via parallel format. A 30 MHz surface mount TCXO oscillator from STC is used as the reference clock and a Mini-Circuits T1-1T Transformer is used to match the output of the DDS to 50Ω . The DDS implementation is shown in Figure 6.6.

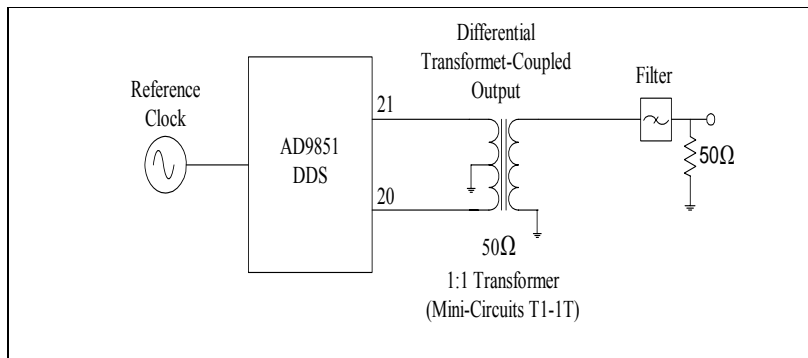


Figure 6.6 DDS configuration.

The relationship between the output frequency, system clock and tuning word of the AD9851 is determined by the following expression:

$$f_{out} = \frac{(\Delta Phase \times SystemClock)}{2^{32}} \quad (6-4)$$

The DDS will be used to generate the sweep frequency of the VCO by sweeping the output frequency of the DDS accordingly. This means that the speed at which the DDS's output frequency can be changed, will determine the maximum modulation frequency of the VCO. The DDS frequency increments are dependent on the speed at which the DDS can change its output frequency and the time it takes from programming the new frequency word.

The DDS output generates a lot of high order harmonics. It is therefore essential to use a filter at the output of the DDS to get rid of these high order harmonics. The next section looks at the filter implementations.

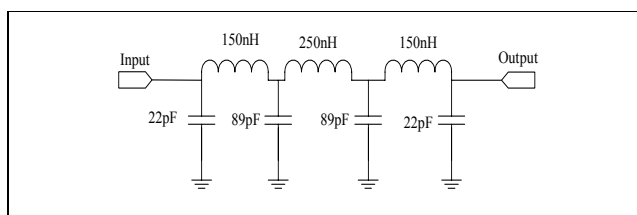
6.5 Filter Implementation

The filter at the DDS output is designed by using Micro Wave Office's [20] filter design wizard. The following specification was used to design the filter.

Table 6.2 Filter specifications

<i>Filter Type</i>	Butterworth LPF
<i>Filter order</i>	7
<i>Band Edge Frequency</i>	60 MHz
<i>Pass Band Ripple Value</i>	0.5 dB
<i>Load Resistance</i>	50 Ω
<i>Source Resistance</i>	50 Ω

The following figure shows the filter after the values of the components were changed to realisable values.

Figure 6.7 7th Order Butterworth Low Pass Filter.

The following figure shows the response of the filter.

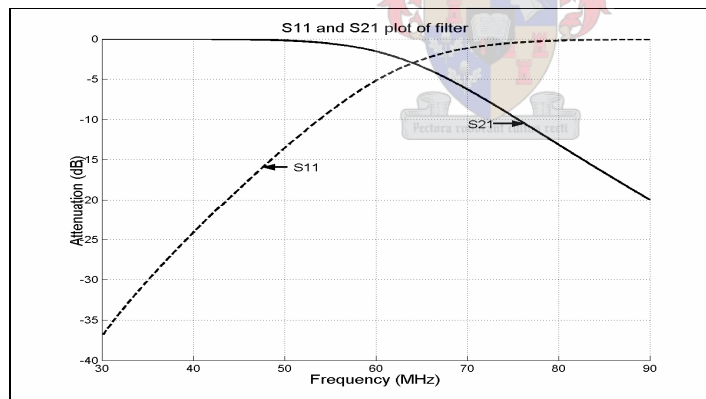


Figure 6.8 Measured frequency response of filter.

Probably the most important part of the PLL is the loop filter. This filter will determine the speed at which the loop can track changes in the reference frequency, and will thus determine the system bandwidth and the modulation discussed in section 5.4. For this implementation the first order lag-lead LPF shown in Figure 6.9 is used because of the stability advantages above the first order LPF (see section 5.4.3).

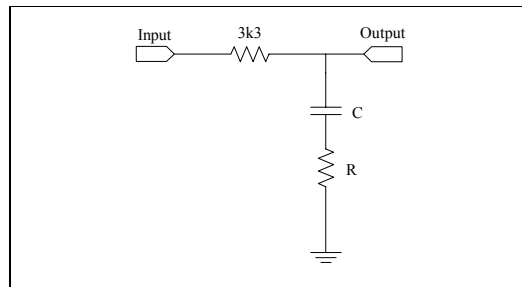


Figure 6.9 LPF configuration.

The values of $C = 1\mu F$ and $R = 320\Omega$ were calculated using equation 5-23 and theory discussed in section 5.4. Figure 6.10 shows a simulation of the LPF frequency response.

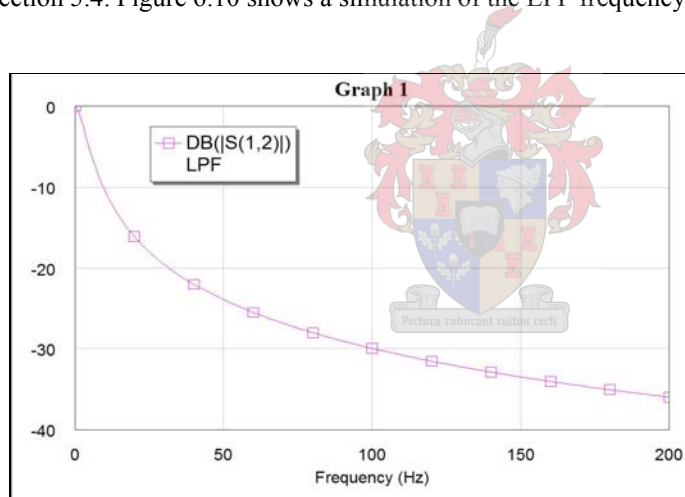


Figure 6.10 Simulation of LPF frequency response [20].

6.6 Microcontroller Implementation

The microcontroller implementation is done by using an ATmega8 chip. The function of this microcontroller is to programme the ADF4113 and the AD9851.

6.7 Implementation and Measurements of PLL

The 94.5 GHz VCO was downconverted too an IF of between 2 and 3 GHz and used in the PLL with DDS as reference. The VCO output signal was locked to the DDS reference and measurements were made using the following test setup:

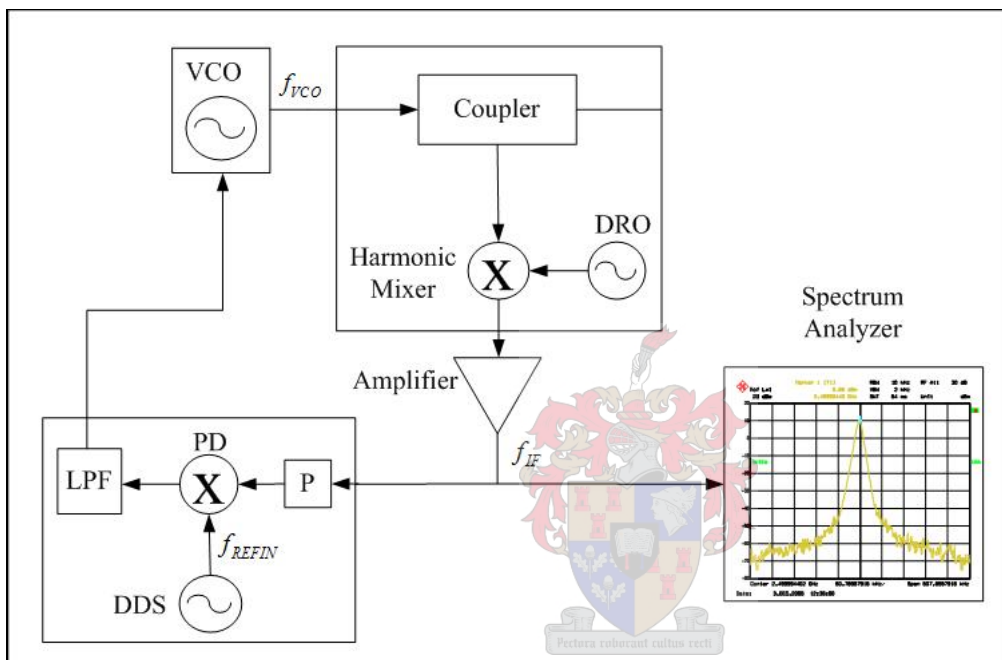


Figure 6.11 Test Setup used to do measurements on locked VCO output.

For $f_{IF} = 2.5\text{GHz}$, $f_{REFIN} = 20\text{MHz}$ and $P = \frac{16}{17}$, the prescaler values are calculated using equation 6.2 to be

$$A = 4, B = 781, \text{ and } R = 100.$$

Figure 6.12 illustrates the spectrum of the locked VCO output signal.

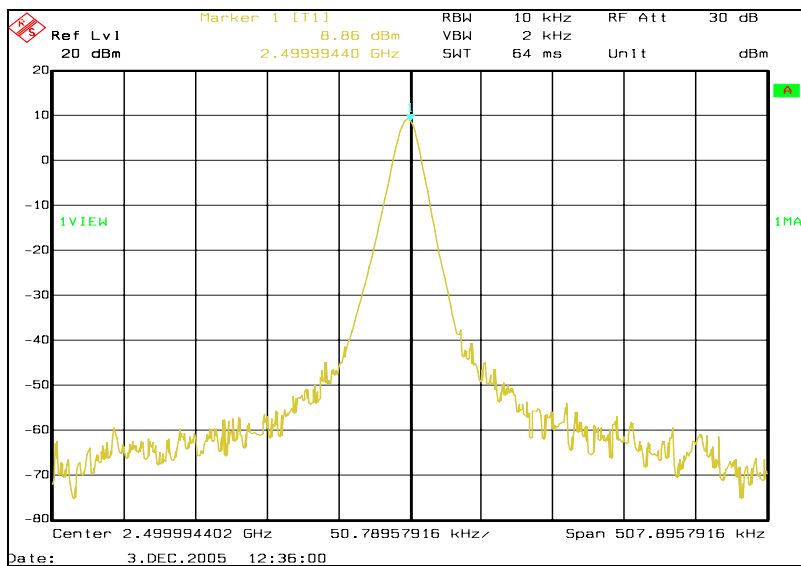


Figure 6.12 Measured output signal of locked VCO.

The above measurement illustrates CW operation. For this application frequency modulation must be applied to the CW signal. To achieve this the frequency of the reference input to the PLL can be modulated. The 94.5 GHz VCO will follow the PLL input reference, assuming that lock is obtained and it can therefore be assumed that the linearity of the 94.5 GHz VCO will be directly proportional to the linearity of the PLL input reference. The linearity of the 94.5 GHz VCO can therefore be obtained by measuring the linearity of the input reference to the PLL.

Lock will be established if the PLL can compensate sufficiently for non-linearities of the 94.5 GHz VCO. To see the effect of the compensation of the PLL the test setup illustrated in Figure 6.13 can be used to measure the frequency-voltage response of the 94.5 GHz VCO.

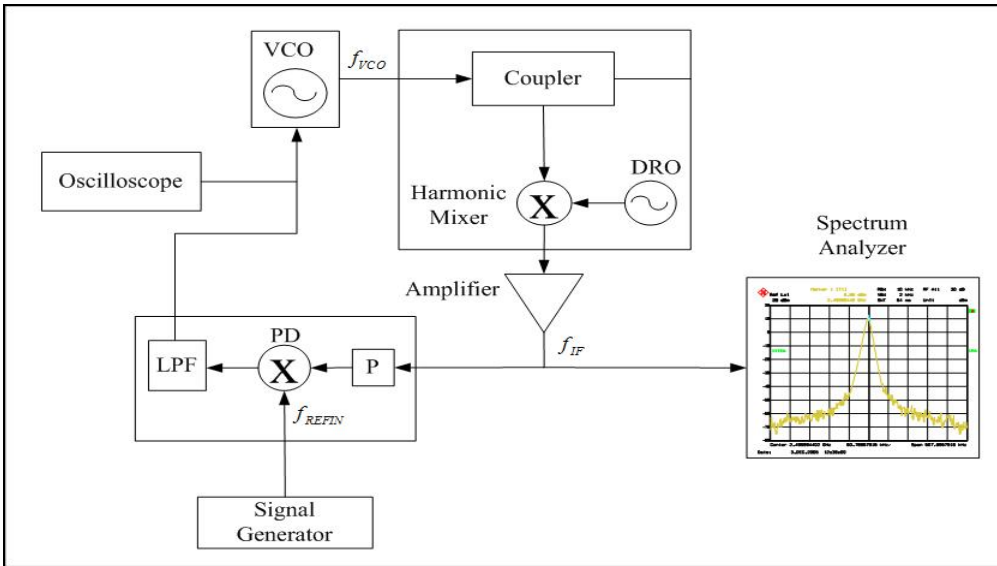


Figure 6.13 PLL compensation test setup.

By manually modulating the output frequency of the DDS, a graph of the 94.5 GHz VCO tuning voltage vs output frequency can be measured and is illustrated in Figure 6.14.

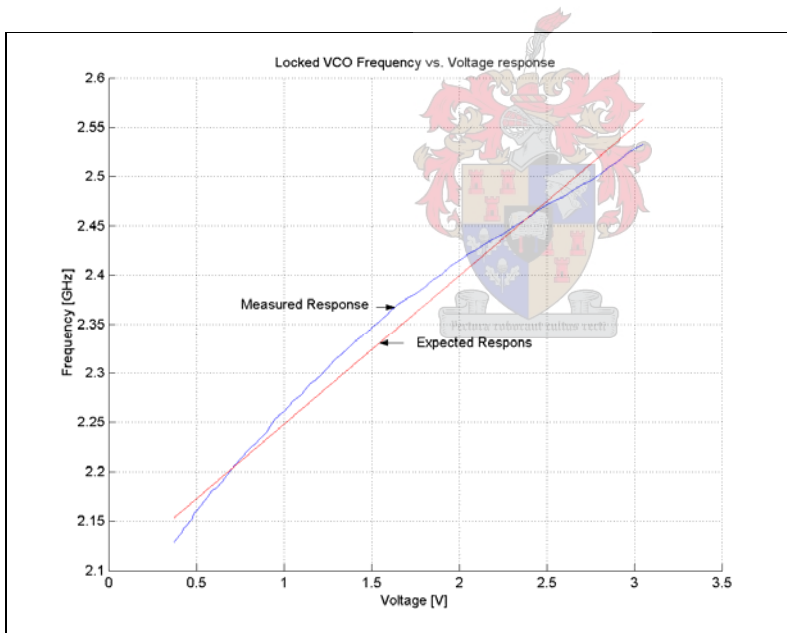


Figure 6.14 Measured frequency-voltage response of FM-CW VCO.

If the VCO was linear, the frequency-voltage response would have been a straight line as indicated by the plot line of the expected response. The measured response plot however, shows clearly how the PLL compensates for non-linearity of the 94.5 GHz VCO.

The final step would now be to determine the improvement in the linearity of the existing system. This is done by measuring and calculating the linearity of the DDS. The following test setup was used to do the measurement of DDS linearity.

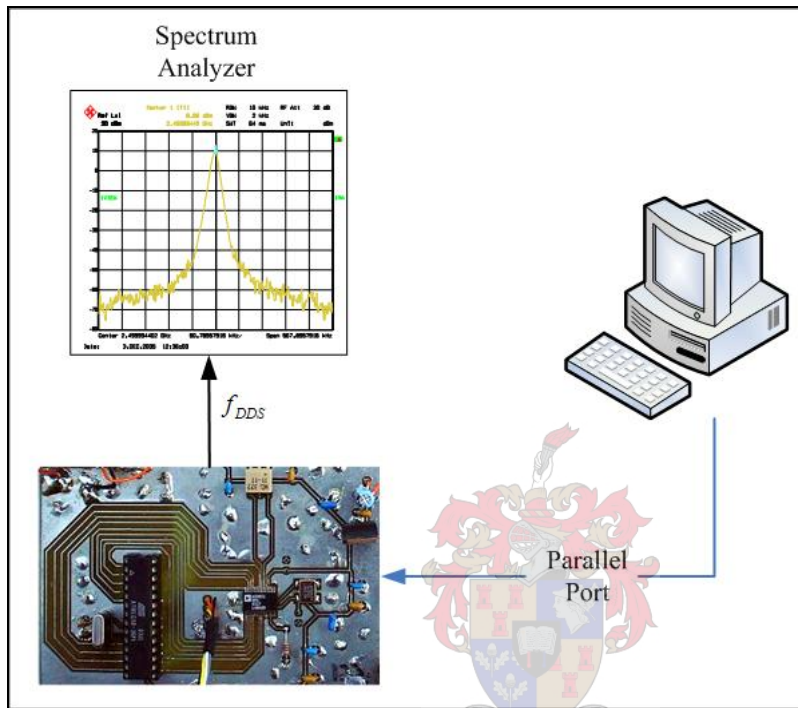


Figure 6.15 DDS Linearity measurement setup.

The measurements were done using the spectrum analyser configured as shown in Table 6.3.

Table 6.3 Spectrum analyser setup.

Span	1 kHz
Resolution Bandwidth	10 Hz
Video Bandwidth	100 Hz
Sweep Time	2 seconds

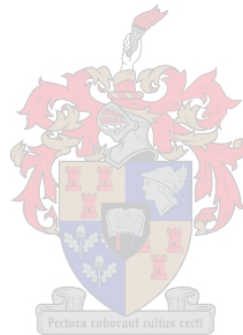
The linearity of the DDS was measured by programming the DDS for specific frequencies and comparing the measured output frequencies with the expected programmed output frequencies. Table 6.4 shows the measured results of the DDS linearity.

Table 6.4 Measured DDS linearity.

f_{prog} [MHz]	f_{meas} [MHz]	Linearity
1	1.000011	0.001%
10	10.000101	0.001%
20	20.0002	0.001%
30	30.000295	0.00098%
40	40.000394	0.00098%
50	50.00049	0.00097%
60	60.0006	0.001%
70	70.0007	0.001%
80	80.00082	0.001%

From this measurement the linearity of the DDS and hence the 94.5 GHz VCO is 0.001%.

This is a clear improvement of the existing system linearity of 3% (section 4.1).



6.8 Conclusion

Figure 6.16 shows the final implementation of the linearisation technique using a PLL with a DDS as reference for locking the VCO.

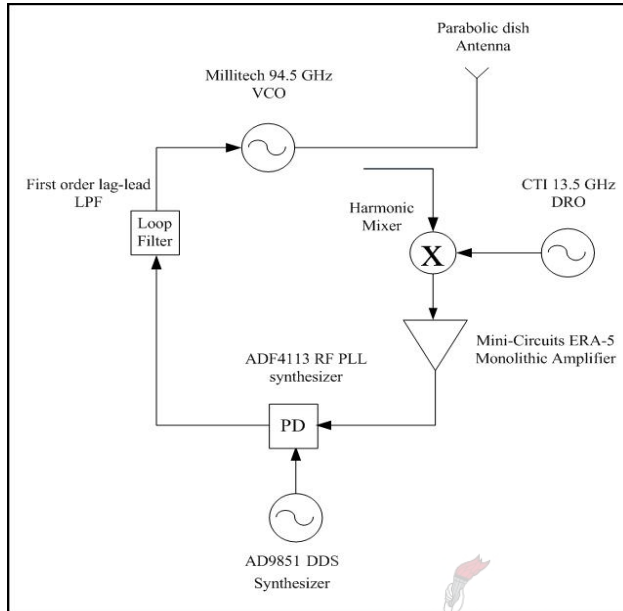


Figure 6.16 Block diagram of 94.5 GHz PLL using DDS technique implementation.

The overall improvement in the performance of the system could be determined by measuring the improvement in the accuracy obtained in target detection. This can be done by placing a corner reflector at different close range distances. By comparing the actual distances from the radar to the corner reflector with the measured distances, the overall system improvement can be calculated. Signal processing in MMW Radar systems is a complicated procedure.

The 94.5 GHz VCO was locked by using the configuration illustrated in Figure 6.16. The linearity of the locked 94.5 GHz VCO was measured as 0.001%. This is a clear improvement in the existing system linearity of 3%.

7 Conclusions and recommendations

7.1 Conclusion

A short introduction to the history and development of MMW radars were introduced with a discussion on the basic fundamentals and environmental factors. MMW radar advantages, namely high angular tracking accuracy, high antenna gain with small aperture, reduced electronic countermeasures vulnerability, reduction in multipath and ground clutter identification were compared with the disadvantages, namely high component cost, low component reliability and availability and short range. The basic functional elements, namely the antenna, quadrature hybrid, coupler, DRO, harmonic mixer, isolator and VCO were discussed and characterised to gain a better understanding on the working of the existing MMW system

A study of the Doppler effect was done to explain the principles used by a CW- and FMCW Radar to detect target speed and distance. The influence of the linearity on the performance and accuracy of the CWFM-Radar is explained by time- and frequency domain simulations of the modulation- and deviation frequency of the system.

Linearisation techniques, namely open loop linearisation, closed loop linearisation and PLL using a DDS are introduced with a detailed discussion of each technique. Open loop linearisation is relatively inexpensive and an easy technique to use. The open loop technique will however not be able to correct or compensate for VCO frequency drifts and unpredictable environmental conditions. To overcome these problems the VCO can be placed in a closed feedback loop. A study of the different closed feedback loop typologies, namely using a digital frequency discriminator, an analog frequency discriminator and a phase-lock loop using a DDS was made. These techniques were compared and the PLL using a DDS was chosen for improving the linearity of the existing system.

A study of the basic principles of a PLL was done to help with the design and implementation of the chosen linearisation technique. PLL operation, lock and capture

requirements, the capture transient and the effect of the loop filter were discussed in detail. Different phase detectors, namely the digital phase detectors, the XOR phase detector, two state phase detector and the phase-frequency detector were introduced and discussed thoroughly. Root locus simulations were done for the different possibilities of low-pass filter designs.

The IF of the mixed down 94.5 GHz VCO had to be amplified to the correct value for the PLL. An 32 dB amplifier was designed and implemented. The 94.5 GHz VCO was locked to the DDS frequency of the PLL.

7.2 Recommendations for future research

The research and development of a new linearisation technique was done to improve an existing one. This new linearisation technique has certain limitations.

Future research may include the following:

- The aim of this research was to improve the linearity of an existing system by improving the linearity of the deviation frequency vs. the modulation time. Phase noise, however, is also an important factor to consider for improving the linearity of the system.
- The DDS is used to modulate the frequency of the CW Radar. Thus, modulation techniques of the DDS signal should be investigated.
- Improvements on the PCB can be made to improve the overall system noise caused by RF leakage on the PCB.
- Improvement of the low-pass filter can also be done to improve the lock time and the overall PLL performance.

The implementation of a PLL using a DDS to improve the existing system linearity were researched and documented in detail. The 94.5 GHz VCO was successfully locked to the DDS frequency.

Bibliography

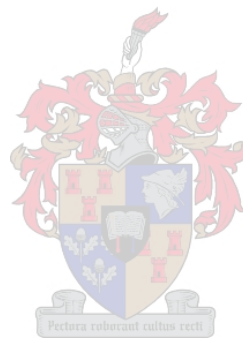
- [1] C.E. Brown and N.C. Currie, "Principles and Applications of MMW Radar," *Artech House*, pp. 3-71, June 1987.
- [2] Merrill I. Skolnik, "Introduction to Radar Systems," *McGraw-Hill Book Company*, New York, pp. 56-57, 68-100, 1962.
- [3] Warren L. Stutzman and Gary A. Thiele, "Antenna Theory and Design," *John Wiley & Sons Inc*, Chapter 1, 1998.
- [4] David M. Pozar, "Microwave and RF Design of Wireless Systems," *John Wiley & Sons Inc*, pp. 547-599, 379, 2001.
- [5] Jacques G. Verly, "Enhanced and Synthetic Vision," *The international Society for Optical Engineering*, 2003.
- [6] Hughes Aircraft Company, "Parabolic Dish Antenna Test Data," March 1991.
- [7] Millitech, "Magic Tee Hybrid Couplers," March 2004.
- [8] Millitech, "3-Port High Directivity Directional Couplers," March 2004.
- [9] OMECON, "DRO Test Data Sheet," *Communication Techniques Inc*, May 1994.
- [10] Hughes Aircraft Company, "Millimeter-Wave Harmonic Mixer Test Data," September 1991.
- [11] Terabeam, "Series HMI & HMC Isolators & Circulators".
- [12] Millitech, "Voltage-Controlled Gunn Oscillators".
- [13] J. B. de Swardt, "Millitech Report".
- [14] N.D. Geldenhuys, "Microwave Frequency Discriminators." Masters, p. 2 March 2001.
- [15] Daniel Abramovitch, "Phase-Locked Loops: A Control Centric Tutorial," 2002.
- [16] David M. Pozar, "Microwave and RF Design of Wireless Systems," *John Wiley and Sons, Inc*, p 226, 274, 2001.

[17] Mini-Circuits, “Optimizing VCO/PLL Evaluations & PLL Synthesizer Designs”.

[18] Mini-Circuits, “Monolithic Amplifiers”.

[19] Program: Matlab 6. The Mathworks, Inc.

[20] Program: Microwave Office 2001. Applied Wave Research, Inc.



Appendix A Range resolution as a function of slope linearity

The slope of the transmitted frequency is:

$$\text{Slope} = \frac{\partial f}{\partial t}$$

The linearity of the slope is:

$$\text{Lin} = \frac{\left(\frac{\partial f}{\partial t}\right)_{\max} - \left(\frac{\partial f}{\partial t}\right)_{\min}}{\left(\frac{\partial f}{\partial t}\right)_{\min}}$$

From the standard FM|CW equation,

$$\frac{f_b}{t} = \frac{\partial f}{t}$$

If the range remains constant then t remains constant and only f_b changes with the slope.

$$\text{Lin} = \frac{\frac{f_{b\max} - f_{b\min}}{t}}{\frac{f_{b\min}}{t}}$$

$$\text{Lin} = \frac{f_{b\max} - f_{b\min}}{f_{b\min}}$$

Also from standard equation $f_b = \frac{2R\Delta f}{Tc}$

$$\Rightarrow \text{Lin} = \frac{R_{\max} - R_{\min}}{R_{\min}} = \frac{\partial R}{R}$$

$$\Rightarrow \partial R = \text{Lin} \cdot R$$

